Shock waves in a transverse magnetic field

A. L. Velikovich and M. A. Liberman

Institute of Physical Problems, Academy of Sciences of the USSR
Usp. Fiz. Nauk **129**, 377–406 (November 1979)

Experimental and theoretical work on ionizing shock waves in a fully ionized plasma is reviewed for the case in which a magnetic field is imposed parallel to the plane of the shock front. The boundary conditions for ionizing shocks are discussed. It is shown that the additional boundary conditions required for ionizing shock waves follow from the ionizational stability of the gas ahead of the shock front. The front structure of ionizing shocks is analyzed qualitatively: some calculated results are also reported. Experimental results on magnetic structures are discussed. The physical mechanisms which shape the shock front in a plasma are examined. Some results calculated for the front structure in a plasma are reported.

PACS numbers: 52.35.Tc

CONTENTS

I. INTRODUCTION

The theoretical and experimental research on this problem is motivated by the many applications in astrophysics, aerodynamics, and various laboratory experiments and devices in which shock waves appear in a magnetic field.

Shock waves are produced by novae, collisions of galaxies, etc., and they are produced in the geomagnetic field by lightning or when manmade satellites or meteoroids enter the ionosphere.

In the laboratory, shock waves arise in magnetic fields in z pinches, θ pinches, reverse pinches, electromagnetic shock tubes, and plasma-focus devices; during gas breakdown by an electric discharge; and in the irradiation of a target with, or gas breakdown caused by, a focused laser beam.

Strong shock waves ionize and heat gases. From the stand-point of the effort to produce hot plasma for the fusion effort, collisional shock waves in dense plasmas have the attractive feature that most of the dissipated energy is transferred to ions. Then it is not necessary to deal with the problem of transferring energy from electrons to ions—a serious problem at high temperatures in traditional ohmic-heating devices.

Much progress has recently been made in producing dense, hot plasmas by shock heating.[1,2] The hydrogen plasmas produced by focusing shock waves in electromagnetic shock tubes with a transverse magnetic field typically have the properties $T_i \sim 1$–2 keV, $T_e \sim 100$ eV, and $N \sim 10^{16} - 10^{17}$ cm^{-3}. The velocity of the shock front ranges up to $5 \cdot 10^8$ cm/sec, and the initial gas pressure and temperature are $p_1 = 0.05$ torr and $T_1 = 293$°K. The acoustic Mach numbers is about 3000, while the Alfvén Mach number is a few tens. The transverse magnetic field in these devices is important not only for thermal insulation but also for forming much narrower shock fronts, so that the device itself can be smaller than it would have to be in the absence of a magnetic field.[3–5]

Several reviews of collisional shocks in magnetic fields have been published.[6,7] Since their publication, many new experimental and theoretical results have been obtained, which can be used to draw a more detailed picture of the physics of the interaction of shock waves with magnetic fields.

This interaction is pertinent to an extremely large number of situations: the shock heating and confinement of plasmas, the dynamics of MHD channel flow, the interaction of shocks with inhomogeneities of the medium, etc.[8–17] The solution of these problems requires a clear understanding of the physics of shock waves in magnetic fields, particularly on understanding of the role played by various physical processes which affect the front structure and of which structures can form. Systematic study of shock waves in magnetic fields began in the late 1950s, when the first high-power electromagnetic shock tubes were constructed.[18–20] The operation of an electromagnetic shock tube is basically the same as that of an ordinary shock tube. A high-current discharge at one end of the tube causes rapid ohmic heating of the gas, which results in an abrupt pressure in-

 0038-5670/79/110843-17$01.10

crease, similar to that which occurs in an explosion. The shock wave which forms as a result propagates toward the other end of the tube. The most promising version of an electromagnetic shock tube is that in which there is a magnetic piston, in which case the pressure drop is intensified by virtue of the magnetic pressure of the magnetic field produced by the discharge current. The magnetic pressure in these devices reaches hundreds of atmospheres for currents in the magampere range.

We wish to emphasize at this point that it is in a plasma, especially a laboratory plasma, in which an understanding of the structure of the shock front is important for understanding the shock behavior. In a neutral gas, a shock wave (in the absence of slow relaxation processes) can be approximated quite accurately as an actual discontinuity, since the front width, on the order of the mean free path of a gas atom or molecule, is generally many times smaller than all the characteristic dimensions of the problem, and the states of the gas on the two sides of the front are related unambiguously by the Rankine-Hugoniot relations. In a plasma, things become more complicated: Even if there is complete thermodynamic equilibrium on the two sides of the shock front, the conservation laws from which the Rankine-Hugoniot relations are derived no longer give the jumps in all the quantities at the front. For example, the conservation laws contain no information on the two-fluid nature of the plasma, on the possibility of charge separation at the front, or on the resulting formation of an axial electric field. In collisional shocks, this charge separation is usually slight, and the plasma can be treated as quasineutral in a first approximation (and we will adopt this approximation everywhere below, except where otherwise specified). The jump of the electric potential at the front due to the axial field, however, is too large to be ignored; its value is not given by the conservation laws, but depends on the front structure. Furthermore, in actual experiments the situation behind the front is frequently not a complete equilibrium: It may be that the temperature or ionization relaxation is still in progress; the nonequilibrium plasma behind the front may be beginning to interact with the magnetic piston; and so forth. For ionizing shock waves, the Rankine-Hugoniot relations themselves cannot be written unless something is known about the structure (more on this below). The net result is that what actually occurs in the experiment has little in common with the narrow discontinuity in an ideal gas; the actual shock wave is more likely to be broad (with a width comparable to the dimensions of the device itself), to have a transition region, and to be "thick." To interpret the experimental results, furthermore, it is crucial to understand precisely which physical mechanisms are responsible for shaping the front structure. The natural way to approach this question is to study steady-state structures, and such structures are the subject of the present review.

We will discuss the theoretical and experimental results on the physics of transverse shock waves, by which we mean shock waves for which the external magnetic field is directed parallel to the plane of the wave front. In Part II we will discuss transverse ionizing shock waves. We will examine the problem of formulating the boundary conditions for ionizing shock waves in magnetic fields. We will show that, in addition to the boundary conditions, which follows from the conservation laws, there is another, which results from the requirement of an ionizational stability of the unperturbed neutral gas ahead of the shock front. We will qualitatively analyze the front structure for the case of transverse ionizing shocks, and we will report some calculated results. Experimental work on the structure of ionizing shocks will be discussed.

In Part III we will discuss transverse shocks in a fully ionized plasma. The various physical processes which shape the front structure will be discussed. The experimental results available on strong shocks in plasmas will be examined.

II. TRANSVERSE IONIZING SHOCK WAVES

1. Boundary conditions and ionizational stability

The front structure of a shock wave is described by a system of differential equations. The first question which arises is that of which stationary solutions are allowed by the original system of equations. If we imagine the shock front to be a discontinuity surface of zero thickness, then the stationary solutions (singularities of the system of differential equations) will be related to the so-called Rankine-Hugoniot relations, which are none other than the boundary conditions at the discontinuity surface. The front structure depends on the boundary conditions at the discontinuity surface which are consistent with the original equations. The boundary conditions for a transverse ionizing shock wave are of particular interest, since the conservation and continuity equations are not sufficient for specifying the boundary conditions in this case, in contrast with the case of shock waves without a magnetic field. The nonconducting gas ahead of the shock front does not interact with the magnetic field, while the onset of a finite conductivity at the wave front causes this interaction to come into play. The strength of the magnetic field behind the front obviously depends on whether this interaction is important at the beginning or end of the shock front. In the former case, more of the wave energy will be expended on magnetic compression, so that the temperature, gas density, etc., will be lower behind the front in the final state. The magnetic field, the temperature, and the gas density behind the shock front are thus not governed unambiguously by the conservation laws, as they are in the case of shock waves without a magnetic field; instead, they depend on the front structure. This structure depends in turn on the boundary conditions. Aside fron the boundary conditions which we obtain from the energy and momentum conservation equations and the continuity equation, there must be one more algebraic relation among the variables which characterize the flow on the two sides of the shock front. From the very fact that transverse ionizing shock waves do exist in nature it follows that the solution of the corresponding equations must be stable, or—almost equivalently—the shock wave must

be "evolutionary."[21] For the wave to be evolutionary, the total number of small-amplitude waves which propagate away from the front must be one fewer than the number of boundary conditions,[21] or, loosely, the number of independent algebraic relations at the discontinuity surface must be equal to the number of independent variables characterizing the flow. In this case, these variables are the density ρ, the velocity v, the temperature T, and the magnetic field H.

Several workers[22-25] have attempted to find the additional boundary condition by examining the front structure. They worked entirely from the MHD equations, assuming the gas to be in thermodynamic equilibrium, and ignoring the ionization equation. Although, in principle, this approach can be effective, its applicability is severely limited.

Let us write the equations for a transverse ionizing shock wave in the coordinate system in which the shock front is at rest. Then for a stationary plane wave which is propagating along the x axis in an ideal gas ($\gamma = 5/3$) with a magnetic field $\mathbf{H} = \{0, 0, H\}$ we have

$$\frac{dH}{dx} = \frac{4\pi\sigma}{c}\left(\frac{vH}{c} - E_y\right), \qquad \frac{dE_y}{dx} = 0, \tag{1.1}$$

$$\frac{d(nv)}{dx} = q_i - q_r, \tag{1.2}$$

$$Nv = C, \tag{1.3}$$

$$MNv^2 + NT + nT_e + \frac{H^2}{8\pi} = P, \tag{1.4}$$

$$\frac{1}{2}MNv^3 + \frac{5}{2}NTv + \frac{5}{2}nT_ev + \frac{c}{4\pi}E_yH + Jnv = S, \tag{1.5}$$

$$\frac{3}{2}nv\frac{dT_e}{dx} + nT_e\frac{dv}{dx} = \frac{c^2}{16\pi^2\sigma}\left(\frac{dH}{dx}\right)^2 - \left(J + \frac{3}{2}T_e\right)\frac{dnv}{dx} + Q_\Delta \tag{1.6}$$

Equations (1.1)–(1.6) are, respectively, Maxwell's equations, the ionization equation, the continuity equation, the conservation equations for the momentum and energy flux for the gas as a whole (electrons, ions, and atoms), and the heat-transfer equation for electrons. Here σ is the conductivity, M is the mass of the atom or ion, N_a and n are the number densities of atoms and electrons (or ions), respectively, $N = n + N_a$, J is the ionization potential, Q_Δ is the heat transferred to electrons in elastic collisions with atoms and ions, q_i and q_r are the numbers of events in which electrons are produced and lost, and C, P, and S are integration constants.

In the comoving coordinate system there is a flow of neutral gas from $x = -\infty$ [singularity 1 of system (1.1)–(1.6)] with a velocity v_1, a temperature T_1, and N_1, and a magnetic field H_1. Behind the shock wave, at $x = +\infty$ (singularity 2), there is a flow of ionized gas, with velocity v_2, density N_2, temperature T_2, etc.

Since the gas behind the shock front has a finite conductivity σ_2, it follows the vanishing of the transverse current, the consequent vanishing of the electric field in the gas coordinate system, and (1.1) that

$$E_{y1} = E_{y2} = \frac{v_2H_2}{c}. \tag{1.7}$$

The results of Refs. 22–25, based on the so-called T^* model, can be summarized as follows: If we transform to the variables $\omega = v/v_2$ and $h = H/H_2$ and eliminate the density and temperature from Eqs. (1.3)–(1.5), we find some function $\Phi(h, \omega) = 0$. The singular points 1 and 2

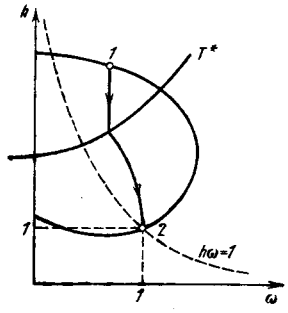

FIG. 1. Integral curve illustrating the structure of the shock wave.[23]

obviously belong to the curve $\Phi(h, \omega) = 0$, shown in the (h, ω) plane in Fig. 1. The final state (point 2, which has the coordinates $h = 1$, $\omega = 1$ in terms of these variables) is the intersection of the $\Phi(h, \omega) = 0$ curve and the hyperbola $h\omega = 1$. [The second point at which the hyperbola intersects the curve $\Phi(h, \omega) = 0$ corresponds to an MHD shock wave with a zero electric field ahead of the shock front, since in this case we have $v_1H_1 = v_2H_2$.] We now assume that $T = T^*$ is that temperature at which $\sigma(T < T^*) = 0$, while for $T > T^*$ the conductivity has a finite value. Then in principle we can move back along the integral curve from point 2 to the intersection with the $T = T^*$ isotherm, in accordance with Eq. (1.1). Above the $T = T^*$ isotherm, the integral curve is vertical up to its intersection with the $\Phi(h, \omega) = 0$ curve, since here $\sigma(T < T^*) = 0$ (Fig. 1).

In principle, this model will allow us to find point 1 by trial and error through numerical integrations. We see from Fig. 1 that this model has the front of any ionizing shock wave (including an MHD shock wave) beginning from a gas-dynamic discontinuity, beyond which there is a region of magnetic field compression. For magnetic compression in this model (for a change in the magnetic field over a distance on the order of the width of the gas-dynamic discontinuity), the condition

$$\mathrm{Rm}_a = \frac{4\pi\sigma v_1\Delta}{c^2} \geqslant 1$$

must hold, where $\Delta \sim l_a$ is the width of the viscous discontinuity. This condition, along with the requirement of equilibrium ionization in the shock wave $\Delta_{ion} \ll c^2/4\pi\sigma v_1$, leads to an extremely severe restriction on the applicability of the model. From these inequalities we find the following for the acoustic Mach number:

$$1 \leqslant \mathrm{M}_1 < \sqrt{\frac{M}{m}\frac{\sigma_{ion}}{\sigma_{aa}}},$$

where σ_{ion} and σ_{aa} are the cross sections for ionization and for atom-atom collisions. The restriction $\mathrm{Rm}_a \geq 1$, which has essentially no range of applicability, is linked to a seemingly paradoxical result, which was found by Hoffert.[26] In accordance with the conclusions based on the T^* model and a numerical integration of a realistic system of equations, Hoffert concluded that only trivial magnetic structures, without magnetic compression, would be possible.

Somewhat later, Leonard[108] carried out an exhaustive study of a model of ionizing shock waves beginning from a gas-dynamic discontinuity and showed that under the condition $\mathrm{Rm} < 1$ there could be only a trivial magnetic

structure for a transverse shock wave.[109]

The front structure of a transverse ionizing wave[27-29] has been studied experimentally by Vlases,[27-29], Stebbins and Vlases,[30] and Patrick and Pugh.[31] The most-detailed work was that by Vlases,[27-30] who used a reverse pinch with an external magnetic field directed along the pinch axis. The operation of that device was extremely simple: A discharge near the pinch axis forms a cylindrical current sheath, which moves radially away from the axis at a high velocity because of the magnetic pressure of the magnetic field produced by the return current through the central conductor at the pinch axis. This current sheath acts as a piston, forming a shock wave ahead of itself. The piston velocity and the velocity of the shock front are essentially constant during a linear increase in the discharge current. The reverse pinch has several advantages over other devices for studying shock waves. In addition to the stability of the shock fronts and the good reproducibility of results, the azimuthal magnetic field H_θ and the electric field E_z of the current sheath of the magnetic piston are orthogonal to the shock-compressed field H_z and to the front-generated electric field E_y in a reverse pinch. As a result, the shock front and the current sheath of the piston are always resolved well in electric and magnetic measurements. The experiments by Stebbins and Vlases[30] were carried out especially to study the magnetic structure of a transverse ionizing shock wave and to test the T^* model. The outside diameter of the tube in their experiments on reverse pinches was 45 cm; the diameter of the inner electrode was 2.5 cm, and the height was 15 cm. A voltage of up to 30 kV was applied to the electrodes; the discharge current pulse was 10 μsec long; and the external magnetic field was $H_1 = 0-4$ kOe. The experiments were carried out in hydrogen at 0.25 and 0.1 torr. Vlases also used argon in some earlier experiments.[27-29] Using magnetic probes to measure the magnetic compression across the shock front for various front velocities, they concluded that there was a qualitative agreement with the conclusions of the T^* model.[30] At low front velocities, $v_1 = (4-5)\times 10^6$ cm/sec, no magnetic compression was observed ($H_2/H_1 = 1$), while at high velocities, $v_1 \gtrsim 8\cdot 10^6$ cm/sec, the compression corresponded to an MHD shock wave (i.e., $H_2/H_1 = \rho_2/\rho_1$). By itself, this qualitative comparison between the experimental results and the predictions of the T^* model is trivial and fails to confirm the theory, since at low front velocities in the experiments by Stebbins and Vlases the magnetic Reynolds number was $\mathrm{Rm} \leqslant 1$, so that $H_2/H_1 = 1$, while at higher front velocities the ionization energy of the gas was negligibly small in the energy balance for the shock wave, and the shock wave had a clearly MHD structure. We pointed out that on all the oscilloscope traces shown in the paper by Stebbins and Vlases the magnetic compression preceded the pressure pulse (measured with piezoelectric gages), in direct contradiction of the predictions of the T^* model regarding possible front structures.

To explain the magnetic compression observed in Ref. 30 and to find the additional boundary condition explicitly, we proposed the principle of ionizational stability of the gas ahead of the shock front.[32] Since the electric field in the coordinate system of the shock front is given by (1.7), by transforming to the laboratory system we find the following for the electric field in the neutral gas ahead of the shock front:

$$E_y^* = \frac{1}{c}(v_1 H_1 - v_2 H_2). \tag{1.8}$$

It follows from Eqs. (1.3)–(1.5) (see also Fig. 1) that magnetic compression in a shock wave is possible from $H_2 = H_1$ to $H_2 = (v_1/v_2)H_1$. The electric field ahead of the front varies from a maximum $E_y^* = (v_1 - v_2)H_1/c$ to zero at maximum magnetic compression, $v_2 H_2 = v_1 H_1$ (an MHD wave). The neutral gas ahead of the shock front obviously cannot withstand an arbitrarily strong electric field. At a certain field level, electric breakdown occurs, and the gas conductivity increases over some finite time; i.e., this type of flow is unstable. The motion of an ionizing front is stable when the electric field ahead of the shock front has a level which corresponds to a constant gas conductivity in this region.

Equations (1.2) and (1.6) in the gas at rest ahead of the shock front can be written

$$\sigma E^{*2} = n\nu_{\mathrm{ion}}(T_e)\left(J + \frac{3}{2}T_e\right) + \delta n_e \nu_{ea}(T_e - T_a), \tag{1.9}$$

$$\frac{d\alpha}{dx} = \alpha(1-\alpha)\Psi(T_e, N), \tag{1.10}$$

where ν_{ion} is the ionization frequency, ν_{ea} is the frequency of elastic electron-atom collisions, $\alpha = n/N$ is the degree of ionization, and $\Psi(T_e, N)$ is the rate at which electrons are produced; here

$$\Psi(T_e) > 0 \quad \text{for} \quad T_e > T_k,$$
$$\Psi(T_e) = 0 \quad \text{for} \quad T_e = T_k,$$
$$\Psi(T_e) < 0 \quad \text{for} \quad T_e < T_k.$$

It follows from (1.10) that a constant conductivity is provided ahead of the shock front, at $x = -\infty$, if $T_e = T_k$. The electric field corresponding to the value $T_e = T_k$ according to Eq. (1.9) is none other than the threshold for gas breakdown, E_∞. The additional boundary condition which we are seeking can thus be written[32]

$$v_1 H_1 - v_2 H_2 = cE_\infty. \tag{1.11}$$

If

$$v_1 H_1 \left(1 - \frac{v_2}{v_1}\right)\frac{1}{c} \sim \frac{3}{4}\frac{v_1 H_1}{c} < E_\infty,$$

we should set $\alpha = 0$ everywhere up to the gas-dynamic discontinuity; then in this case (1.11) is replaced by

$$H_2 = H_1. \tag{1.11a}$$

The gas ahead of the shock front should be assumed nonconducting if $\mathrm{Rm}_1 = 4\pi\sigma v_1 L/c^2 \ll 1$, where L is the scale length in the flow ahead of the front. Then, in particular, for the model of a shock wave with an infinite plane front, propagating in a gas without an electron loss which is linear in n, the sole boundary condition is $E_\infty = 0$, i.e., $v_1 H_1 = v_2 H_2$.

For a real situation, the calculation of E_∞ should incorporate both the loss of electrons due to diffusion to the wall of the shock tube and the finite time required for the shock front to propagate through the device. Figure 2, from Ref. 32, shows the value of $v_2 H_2/v_1 H_1$ measured in Ref. 30 along with those calculated from

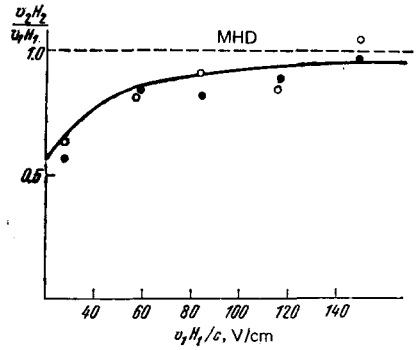

FIG. 2. The quantity v_2H_2/v_1H_1 as a function of v_1H_1/c in an ionizing shock wave.

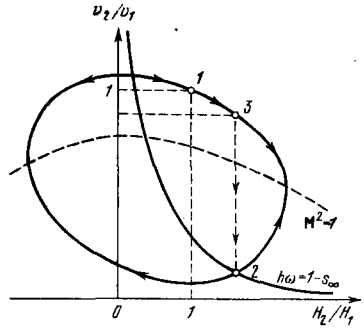

FIG. 3. Structure of the shock wave in the plane of $h=H_2/H_1$ and $\omega=v_2/v_1$ with boundary condition (1.11).

Eq. (1.11). For this example we have selected those experimental results from Ref. 30 which correspond to a constant front velocity v_1; the value of v_1H_1 increases because of the change in H_1. The temperature behind the front (T_2 was calculated from the field compression measured in Ref. 30) in fact decreases as the MHD boundary condition is approached.

Gas breakdown ahead of a shock front in a transverse magnetic field was observed directly by Maksimov and Ostashev.[33] Their apparatus was an explosive shock tube; the working gas was argon, at a filling pressure of 5 torr. The initial field ahead of the front, $E^* \approx v_1H_1/c \approx 150$ V/cm, fell off rapidly to 50 V/cm as the front propagated. Maksimov and Ostashev[33] pointed out that the breakdown is observed at a substantial distance from the wave front, rather than at the maximum of the photoelectron density.

It turns out that in order to solve the boundary-condition problem, which has traditionally been formulated in MHD terms, it is necessary to go beyond MHD: to take into account the production of photoelectrons ahead of the front and the electron breeding in the transverse electric field. In other words, it is necessary to take up the essentially kinetic problem of the unsteady gas breakdown caused by the induced electric field in the actual geometric configuration of the shock tube and in the presence of an electron source (ionizing radiation; "externally sustained" breakdown). Here we might also note that an unexpected close relationship was found betweeen two extremely different experiments with ionizing shock waves: measurement of the compression of a transverse magnetic field and observation of gas breakdown caused by an induced electric field.

2. Structure of the shock front

For a qualitative analysis of the magnetic structure of the front of a transverse ionizing shock wave, we transform to dimensionless variables in Eqs. (1.1)–(1.6):

$$\omega = \frac{v}{v_1}, \quad h = \frac{H}{H_1}, \quad \theta = \frac{T}{T_1}, \quad s_\infty = \frac{cE_\infty}{v_1H_1}, \tag{2.1}$$

where v_1, H_1, and T_1 are the velocity, magnetic field, and temperature ahead of the shock front.

Introducing the acoustic Mach number ($\mathbf{M}_1 = v_1/c_{s1}$) and the Alfvén Mach number ($\mathbf{M}_{a1} = v_1/c_{a1}$) in the free-stream flow, and eliminating the density and temperature from (1.3)–(1.5), we find the equation of the curve on which the initial and final states lie:

$$\Phi(h, \omega) = 4\omega^2 - \omega\left[5 + \frac{3}{\mathbf{M}_1^2} - \frac{5(h^2-1)}{2\mathbf{M}_{a1}^2}\right] + 1 + \frac{3}{\mathbf{M}_1^2} - 2(1-s_\infty)\frac{h-1}{\mathbf{M}_{a1}^2} = 0. \tag{2.2}$$

In terms of the variables in (2.1), the state ahead of the front has the coordinates $\omega = 1, h = 1$, while the state behind the front is the intersection of curve (2.2) with the hyperbola representing a zero electric field in the proper coordinate system of the gas,

$$h\omega = 1 - s_\infty. \tag{2.3}$$

Introducing a local acoustic Mach number, we can derive the following equation from (2.2):

$$\frac{dh}{d\omega} = \frac{3\mathbf{M}_{a1}^2\omega}{5h\omega - 2(1-s_\infty)}\left(\frac{1}{\mathbf{M}^2} - 1\right). \tag{2.4}$$

Curve (2.2) is shown in the (h, ω) plane in Fig. 3; the arrows show the direction which corresponds to increasing entropy, while the dashed curve shows the parabola ($\mathbf{M}^2 = 1$). We see from Fig. 3 that at the shock front there is initially a compression of the magnetic field (regions 1–3); this region gives way to a gasdynamic ($\Delta H = 0$) discontinuity (region 3–2 in Fig. 3) if the acoustic Mach number behind the front is less than unity. More-detailed calculations incorporating the ionization energy of the gas lead to[34]

$$\mathbf{M}_{2cr}^2 = 1 - 4\left[\frac{15(1+\alpha_2)(2-\alpha_2)}{\alpha_2(1-\alpha_2)(J/T_2)^2} + 10\left(1 + \frac{3T_2}{2J}\right)^2\right]^{-1}, \tag{2.5}$$

where α_2 and J are the degree of ionization of the gas behind the front and the ionization potential of the gas, respectively.

If $\mathbf{M}_2 > \mathbf{M}_{2cr}$, the shock structure is governed entirely by ohmic (Joule) dissipation, while when $\mathbf{M}_2 < \mathbf{M}_{2cr}$ there cannot be a continuous transition from 1 to 2 because of ohmic dissipation alone, and an isomagnetic discontinuity in the velocity, the density, and the temperature occurs within the front. The occurrence of an internal isomagnetic discontinuity in an intense shock results from the fact that the energy density dissipated by the current cannot exceed a value on the order of $H_2^2/8\pi$.

The measurements of the electric field behind the front by Stebbins and Vlases[30] apparently constitute an indirect observation of an isomagnetic discontinuity in an ionizing shock wave. The electric field behind the

front is given in the fixed coordinate system by

$$E_2^* = \frac{v_1 H_1}{c}\left(\frac{v_1}{v_2} - 1\right)\frac{H_2}{H_1}. \quad (2.6)$$

Stebbins and Vlases measured the electric field with an electrostatic probe[30] consisting of two metal rods in the azimuthal plane of the pinch. From Faraday's law, we have

$$2\pi r \cdot E_\theta = -\frac{2\pi}{c}\frac{\partial}{\partial t}\int_0^r Hr'\,dr'.$$

Equation (2.6) follows from this equation if the ionizing front is thin. The values of E_2^* measured in Ref. 30 turned out to be several times smaller than those calculated from Eq. (2.6) with the value of H_2 measured by the magnetic probes or calculated from the measured density jump at the front (if we accepted the validity of the MHD theory here, we would have $H_2 = H_1\rho_2/\rho_1$). A possible explanation for this pronounced discrepancy is that the readings were taken from the electrostatic probes, not behind the entire front, but behind the wide region of magnetic compression (1–3 in Fig. 3), ahead of the isomagnetic discontinuity. In this case, if the main jump in the velocity in the shock wave is concentrated in the isomagnetic discontinuity (region 3–2 in Fig. 3) then the electric field ahead of it is much weaker than that behind it. The electric field at point 3, ahead of the isomagnetic discontinuity, is

$$E_3^* = \frac{v_1 H_1}{c}\left(1 - \frac{v_2}{v_1}\right)\frac{H_2}{H_1}. \quad (2.7)$$

Calculations[34] from Eq. (2.7) in fact lead to a good agreement with the measured electric field.

In this experiment we are dealing with a "thick" shock wave and a wide zone of magnetic field compression. This is a natural result: Estimates show that the extent of ionization which occurs ahead of a viscous shock because of the interaction of photoelectrons with the induced electric field (Section 3) is low, so that the diffusion length for the magnetic field is comparable to the dimensions of the device, because of the low conductivity. The magnetic compression is played out completely over this diffusion length, and by the end of the compression the electric field in the laboratory system reaches the value in (2.7).

3. Role of radiation in forming the structure of ionizing shock fronts

The energy density and radiation pressure associated with the thermal emission of electromagnetic radiation become comparable to the energy and pressure of the gas in shock waves if the waves are very intense or if the gas density is extremely low.[35] As a rule, the radiation has little effect on the properties of the gas behind the front, so it can be ignored. The situation is completely different in the case of ionizing shock waves in a magnetic field. The photoionization of the gas ahead of the front of an ionizing shock is a governing factor in the magnetic structure of the front.[34, 36, 37]

The actual process by which the precursor forms has been studied in Refs. 38–50. By precursor here we mean the ionization of the cold gas ahead of the shock front which results from either the diffusion of electrons from the hot gas behind the front or photoionization by the electromagnetic radiation emitted by the shock-heated gas. Since electron diffusion is slow in the transverse magnetic field, the formation of the precursor in a transverse shock wave is due primarily to photoionization. In many cases the intensity of the electromagnetic radiation emitted by even a moderately strong shock wave is sufficient to create a photoelectron density ahead of the front sufficient for the formation of a steady-state magnetic structure.[34]

In Ref. 37 we studied the evolution of the initial shock and the formation of the magnetic structure of a transverse ionizing shock wave. If a gas-dynamic shock wave is produced at $t = 0$ by driving a piston into the tube or by some other method, and if this shock wave propagates across the magnetic field, then at $t = 0$ all the properties of the gas at the shock front undergo jumps, except for the magnetic field, since the magnetic Reynolds number is always small in a viscous shock. The electric field in the gas ahead of the front is thus maximal at $t = 0$, when its value is

$$E_{y1}^* = \frac{v_1 H_1}{c}\left(1 - \frac{v_2}{v_1}\right).$$

Let us examine the evolution of the front of a transverse ionizing shock wave, taking into account both the photoionization of the neutral gas by the electromagnetic radiation emitted by the shock-heated gas behind the front and the impact ionization which occurs in the induced electric field $E_{y1}^* > E_\infty$. The particular behavior of the spectral radiation density behind the front and of the coefficient for electron-impact ionization depends on the nature of the gas, so that numerical methods must be used for a quantitative solution of the evolution problem. We turn now to a qualitative theory for this evolution which reflects all the details of the process.[37]

We assume that the electromagnetic radiation emitted by the hot gas behind the shock front, with temperature $T_2 \ll J$, is approximately the same as that emitted by a blackbody (this assumption is supported by experimental results). Then the flux density of ionizing photons with $\hbar\omega \geq J$ is given by the following equation, which holds up to small terms of order $T_2/J \ll 1$:

$$S_p = \frac{J^2 T_2}{4\pi^2 c^2 \hbar^3} e^{-J/T_2}. \quad (3.1)$$

The electron density produced ahead of the shock front by the photon flux in (3.1) is

$$n = \frac{S_p}{v_1} e^{x/l_p},$$

where $l_p = 1/N_1\sigma_p$ is the mean free path of the ionizing photons, and σ_p is the photoionization cross section.

Let us examine a linearized balance equation for the number of particles in the free stream ahead of the shock front.

If the degree of ionization is $\alpha \ll 1$ we have

$$\frac{\partial \alpha}{\partial t} + v_1\frac{\partial \alpha}{\partial x} = v_1\frac{\alpha}{\Delta_{ion}(T_{e1})} + v_1\frac{\alpha_0}{l_p}e^{x/l_p}; \quad (3.2)$$

here $\Delta_{ion}(T_{e1})$ is the scale dimension of the electron-impact ionization with the electron temperature T_{e1}, which is the temperature the electrons acquire in the

electric field E_{y1}^* ahead of the front.

The solution of Eq. (3.2) with the initial condition $\alpha(x=0)=0$ is

$$\alpha(x,\ t)=\frac{\alpha_0}{|l_p/\Delta_{ion}(T_{e1})|-1}\exp\left(\frac{x}{l_p}\right)\left\{\exp\left[v_1\left(\frac{1}{\Delta_{ion}(T_{e1})}-\frac{1}{l_p}\right)t\right]-1\right\}. \tag{3.3}$$

It can be seen from (3.3) that a steady-state solution is reached in the limit $t\to\infty$ if $\Delta_{ion}(T_{e1})>l_p$. This inequality is a restriction on the electric field ahead of the shock front: As E_{y1}^* decreases, the quantity $\Delta_{ion}(T_{e1})=v_1/(\nu_{ion}-\nu_L)$, ($\nu_{ion}$ is the ionization frequency, and ν_L is the frequency of the electron loss which is linear in n) increases and becomes infinite at $E_{y1}^*=E_\infty$. We thus find a lower limit on the magnetic compression for which there is a solution. The inequality $\Delta_{ion}(T_{e1})>l_p$ can be put in the form

$$1-\sqrt{A\frac{N_1}{M_1}}\leqslant\frac{v_2H_2}{v_1H_1}\leqslant 1, \tag{3.4}$$

where M_1 is the acoustic Mach number, and A is a constant governed by the gas properties. It can be seen from (3.4) that for intense shocks, i.e., in the limit $M_1\to\infty$, the magnetic compression is clearly at its maximum level; i.e., $H_2/H_1=v_1/v_2=\rho_2/\rho_1$. If the electric field ahead of the front is strong, i.e., if $\Delta_{ion}(T_{e1})<l_p$, there is no steady-state solution. In this case Eq. (3.3) represents an ionization wave which is propagating upstream with a phase velocity $v_1[l_p/\Delta_{ion}(T_{e1})-1]$ with respect to the shock front. The propagation velocity of the ionization wave increases with increasing E_{y1}^*, and the degree of ionization increases more rapidly. The high velocity of this wave in comparison with other results for ionization waves in a transverse electric field[51,52] results from the fact that the "seed" electrons are provided by photoionization, rather, than by diffusion.

We see that the formation of the steady-state front structure of an ionizing shock is governed by the instability which occurs in the unperturbed gas ahead of the front, which we mentioned in the Introduction. In this unperturbed gas, the shock wave simultaneously produces photoelectrons and an induced transverse electric field. In the linear approximation, this instability can be described as an ionization wave which detaches from the front. On the basis of Eq. (3.2), of course, we can reach only qualitative conclusions, indicating only tendencies in the evolution of the process. A complete description of the change in the front structure at the transition to the steady state would require the numerical solution of a complicated, nonlinear, time-dependent problem. In particular, as was pointed out at the end of Section 1, a kinetic approach must be taken to find a description of the initial stage of the instability (breakdown), since the electron distribution function in a weakly ionized gas in an electric field is quite different from a Maxwellian distribution, and the concept of an electron temperature generally cannot be used.

4. The shock adiabat. Front structure and ionizational relaxation

For specific calculations of the gas properties behind the front it is necessary to consider the energy expended in ionizing and dissociating the gas. Calculating the velocity (or density) jump from, for example, Eqs. (1.3)–(1.5) and (1.11), we find

$$\frac{v_2}{v_1}=\frac{N_1}{N_2}=\frac{1}{8(\varkappa+1)}\left[1+\frac{3}{M_1^2}+\frac{5+4\varkappa}{2M_{a1}^2}+\sqrt{\left(1+\frac{3}{M_1^2}+\frac{5+4\varkappa}{2M_{a1}^2}\right)^2+\frac{8(\varkappa+1)(4\varkappa+1)}{M_{a1}^2}}\right]. \tag{4.1}$$

Here $\varkappa=\alpha_2 J/2T_2(1+\alpha_2)$ is a parameter which is a measure of the effect of ionization on the velocity jump and the compression in the shock wave. The ionization has a negligible effect only in the case of a weak shock, $\alpha_2\ll 1$, or a very strong shock, $J/T_2\ll 1$.

As the gas density is reduced, $\varkappa$ increases without bound, and the compression which occurs in the shock wave is generally also unbounded. In Ref. 34 we calculated the properties of the gas in a transverse ionizing shock, taking inelastic processes into account. Figure 4, taken from Ref. 34, shows the temperature, the velocity, the degree of ionization, and the degree of dissociation as functions of the acoustic Mach number M_1 for the case of hydrogen.

For an ionizing shock wave, the equation of the shock adiabat is

$$\frac{p_2}{p_1}=\frac{1+\alpha_1}{(1+\alpha_2)(4\omega_2-1)}\left[4-\omega_2+\frac{(1-\omega_2)^2}{\beta_1\omega_2}-2\frac{J}{T_1}\frac{(\alpha_2-\alpha_1)}{1-\alpha_1}\right], \tag{4.2}$$

where

$$\omega_2=\frac{N_1}{N_2},\quad \beta_1=\frac{8\pi p_1}{H_1^2}.$$

If the energy expended on ionization is negligible, Eq. (4.2) becomes the same as the equation for the shock adiabat in a fully ionized plasma.[53]

The problem of the front structure of a transverse ionizing shock was studied on the basis of multifluid hydrodynamics in Ref. 34, where both analytic and numerical solutions were found. Figures 5 and 6, from Ref. 34, show the changes in the magnetic field, the velocity, the temperature, and the degree of ionization in a shock wave in argon for the case $M_2<M_{2cr}$ (Fig. 5) and for the case $M_2>M_{2cr}$ (Fig. 6). All the quantities are given in dimensionless form: $h=H_2/H_1$, $\omega=v_2/v_1$, $\theta=T/T_1$, $\theta_e=T_e/T_1$. The changes in the temperature, den-

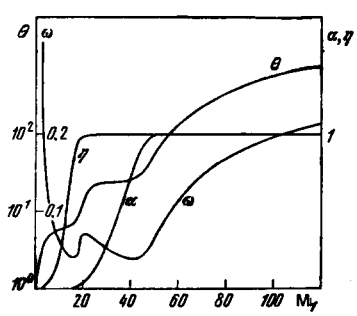

FIG. 4. Variation of the temperature $\theta=T_2/T_1$, the velocity $\omega=v_2/v_1$, the degree of ionization α, and the degree of dissociation η with the acoustic Mach number M_1 in a shock wave in hydrogen.

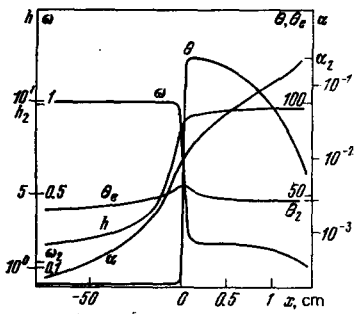

FIG. 5. Structure of the shock front in argon when $M_2 < M_{2cr}$.

sity, velocity, etc., in the shock wave are found by solving the system of differential equations in (1.1)–(1.6) with the appropriate boundary conditions. If we convert to dimensionless variables [defined, for example, as in (2.1)], quantities with the dimensions of length appear in the equations. These quantities are scale lengths of the various physical processes. In particular, from Eq. (1.1) we find the scale length for current dissipation, $\Delta_j = c^2/4\pi\sigma v_1$. This quantity is none other than the scale length for magnetic-field diffusion. The front width in terms of magnetic-field compression is $\Delta_{j1} = c^2/4\pi\sigma_1 v_1$, where σ_1 is the gas conductivity ahead of the front, which arises because of photoionization and which is maintained by the electric field of the shock wave.

It should be noted here that, for the low conductivity of the gas ahead of slow shocks, the observation that there is no magnetic compression in devices of finite dimensions means that a steady-state magnetic structure does not manage to form. The width of the magnetic-compression region produced by photoionization was calculated in Ref. 34 from the value of the conductivity ahead of the front; the result agrees well with the measurements by Stebbins and Vlases at front velocities above $6 \cdot 10^6$ cm/sec, in experiments in which a substantial magnetic compression was observed. At lower velocities, according to Fig. 11 of Ref. 34, the quantity Δ_{j1} is appreciably larger than the dimensions of the device.

Since the rate of impact ionization increases exponentially with the temperature, it is convenient to single out two limiting cases: that of moderately strong shock waves, in which the ionization rate is much lower than the rates of all dissipative processes, and that of strong shock waves, in which the ionization rate almost immediately becomes much higher than the rates of all dissipative processes. In other words, the ionization scale length in the former case is much larger than all the other scale lengths of the problem, while in the latter case it is smaller.

The first of these cases—that of a moderately strong shock wave—is analogous to the detonation-wave model of Zel'dovich and von Neumann. The wave front consists of a thin region of compression and heating (the dissipation zone), which is followed by a much wider relaxation region (the ionization zone). In the relaxation zone, the dissipation is negligible, the density and magnetic field vary only slightly, and the temperature decreases, because of the energy expended on ionizing the gas.

In the opposite limiting case, the ionization at the shock front is so rapid, that a local ionizational equilibrium is attained over the entire shock front, except in an unimportant region at the beginning of the front.

It should be noted that in the case $\varkappa \gtrsim 1$ the basic changes in the velocity, density, and magnetic field occur in the relaxation zone, not in the compression zone.

The thickness of the relaxation zone has been measured for shock waves without a magnetic field. The experiments have been carried out in argon at various filling pressures,[40,53] in mixtures of argon with krypton,[54] and in xenon.[55] The quantity measured experimentally is the ionization rise time τ. Denoting by α_{ion} the coefficient of electron-impact ionization, we find the ionization scale length from (1.2):

$$\Delta_{ion} = \frac{v_2^2}{\alpha_{ion_2} N_1 v_1}.$$

Hence

$$\tau = \frac{\Delta_{ion}}{v_2} = \frac{v_2}{\alpha_{ion_2} N_1 v_1}. \qquad (4.3)$$

A convenient parameter here is the product $p_1\tau$, which varies only slightly with the initial pressure p_1 ($T_1 = 300$ °K):

$$p_1\tau = \frac{T_1 v_2}{\alpha_{ion_2} v_1}. \qquad (4.4)$$

Figure 7 is a plot of $p_1\tau$ against the reciprocal temperature behind the front, found from calculations ignoring the ionization loss. The experimental points, the dot-dashed line, and the solid line are the experimental and numerical results from Ref. 40; the dashed curve is

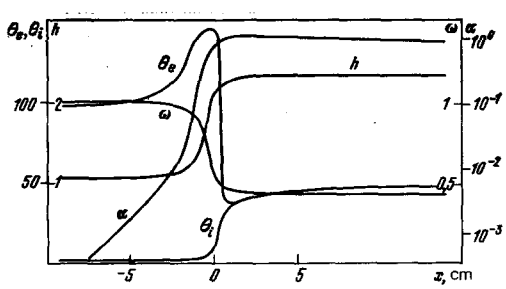

FIG. 6. Structure of the shock front in argon when $M_2 > M_{2cr}$.

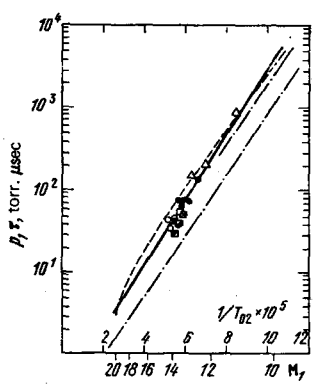

FIG. 7. Ionizational relaxation time for a shock wave in argon.

plotted from Eq. (4.4).

Finally, we should point out that a characteristic structural feature of a transverse shock wave may be a pronounced heating of the electrons in the induced field when the electron temperature and the electron density go through maxima. It is apparently this effect—a maximum in the degree of ionization at the front (nearly an order of magnitude above the equilibrium degree of ionization behind the front)—which was observed in Ref. 31.

III. TRANSVERSE SHOCKS IN PLASMAS

5. Formulation of the problem. Boundary conditions

The structure of transverse collisional shock waves in plasmas has been studied by many workers.[3-5, 56-73] The early theoretical work was based on extremely crude models, but these models have subsequently been refined through the incorporation of a progressively increasing number of physical processes at the front. The problem of the front structure was solved in Refs. 68–70 for weak shock waves on the basis of the Grad 13-moment equation; all the effects consistent with the hydrodynamic approach were taken into account (charge separation, electron inertia, the Hall currents associated with the transport of momentum, energy, charge, etc.). In Refs. 71–73, this work was extended to shock waves of arbitrary intensity through the use of the equations of two-fluid hydrodynamics.[74] Comparison of the results reveals a good agreement, so it appears to be possible to describe the structure of collisional shock waves in plasmas on a purely hydrodynamic basis, without appealing to the higher moments of the kinetic equation. This conclusion is supported by the results of a numerical simulation[3,4] of transverse shocks in plasmas which was based on the hydrodynamic equations with the ordinary plasma transport coefficients.[74,75] The results of these calculations agree well with experiment.[76] It is the two-fluid hydrodynamic description which we will use below.

We consider a steady plane shock wave which is propagating along the x axis in a fully ionized plasma. The z axis is along the magnetic field H. We assume a simple plasma[74] (one ion species with $z=1, \gamma_e=\gamma_i=5/3$). Transforming to the coordinate system of the shock front, we find $E_y = v_1H_1/c = v_2H_2/c$ from Maxwell's equations (see Part II). The equations of the shock layer are the same as in Section 1, but the equations for the transport coefficients correspond to a fully ionized plasma,[74] and ionization and recombination (inelastic processes) do not occur.

The boundary conditions are expressed in terms of the Mach numbers $\mathbf{M}_1$ and $\mathbf{M}_{a1}$ (or $\mathbf{M}_2$ and $\mathbf{M}_{a2}$), which are defined in Section 2. The jumps in the velocity and temperature across the front are

$$\frac{v_2}{v_1}=\frac{N_1}{N_2}=\frac{H_1}{H_2}=\frac{1}{8}\left[1+\frac{3}{\mathbf{M}_1^2}+\frac{5}{2\mathbf{M}_{a1}^2}+\sqrt{\left(1+\frac{3}{\mathbf{M}_1^2}+\frac{5}{2\mathbf{M}_{a1}^2}\right)^2+\frac{8}{\mathbf{M}_{a1}^2}}\right], \tag{5.1}$$

$$\frac{T_2}{T_1}=1+\frac{\mathbf{M}_1^2}{3}\left(1-\frac{v_2}{v_1}\right)\left(\frac{v_2}{v_1}+1-\frac{2}{\mathbf{M}_{a1}^2}\frac{v_1}{v_2}\right). \tag{5.2}$$

Equations (5.1) and (5.2) remain correct when the subscripts are interchanged, $1 \rightleftarrows 2$.

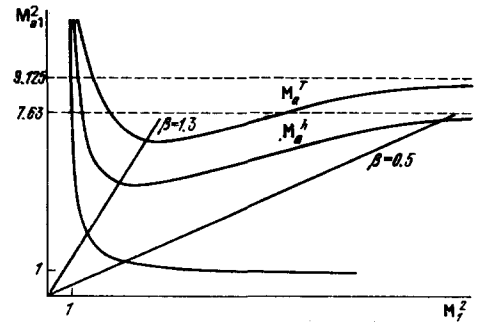

FIG. 8. Ranges of the Mach numbers ($\mathbf{M}_1^2$, $\mathbf{M}_{a1}^2$).

For the motion of a conducting medium across a magnetic field, the MHD description reduces to ordinary hydrodynamics,[77] in which the role of the propagation velocity for small perturbations is played by $c_f=\sqrt{c_s^2+c_a^2}$, the velocity of a fast magnetosonic wave. On this basis we can immediately find the ranges of variation of the Mach numbers $\mathbf{M}_1$ and $\mathbf{M}_{a1}$: Since a shock wave corresponds to supersonic motion in ordinary hydrodynamics, and the condition $v_1>c_{s1}$ holds, we conclude by analogy that we should have $v_1>c_{f1}$ in the present case; i.e., we should have $\mathbf{M}_1=v_1/c_{f1}=\mathbf{M}_1\mathbf{M}_{a1}(\mathbf{M}_1^2+\mathbf{M}_{a1}^2)^{-1/2}>1$ (Fig. 8). Similarly, we should have $\mathbf{M}_2<1$ in the outgoing flow. The corresponding region in the $(\mathbf{M}_2^2, \mathbf{M}_{a2}^2)$ plane lies between the hyperbola $\mathbf{M}_2=1$ and the curve whose parametric equation is

$$\mathbf{M}_2^2=\frac{3\omega_2(5\omega_2+1)}{5(1-\omega_2)^3}, \quad \mathbf{M}_{a2}^2=\frac{\omega_2^2(5\omega_2+1)}{2(4\omega_2-1)}, \tag{5.3}$$

where $\omega_2=v_2/v_1=N_1/N_2$, $1/4<\omega_2<1$. The curve in (5.3) corresponds to the limit of strong shock waves: $\mathbf{M}_1 \to \infty$, $\beta_1=8\pi p_1/H_1^2=(5/6)\mathbf{M}_{a1}^2/\mathbf{M}_1^2 \to 0$ with compression, $\omega_2=\text{const}$ (Fig. 9). In the limit of a low magnetic pressure ($\mathbf{M}_{a2}\to\infty$, $\beta_2\to\infty$), this region converts into the finite interval $1/5<\mathbf{M}_2^2<1$, which corresponds to a shock wave in a gas or plasma without a magnetic field.[78] In the opposite limit of a cold plasma ($\mathbf{M}_2\to\infty$, $\beta_2\to 0$), the interval of permissible values of $\mathbf{M}_{a2}$ contracts to a point, $\mathbf{M}_{a2}=1$. This result is completely natural: The irreversible energy dissipation in the shock wave is due to the compression and heating of the gas component. If the pressure in the final state is low in comparison with the magnetic field pressure, the energy of the free-stream flow is insufficient for gas compression (since the magnetic field is compressed by the same factor), and the shock wave can only be weak.

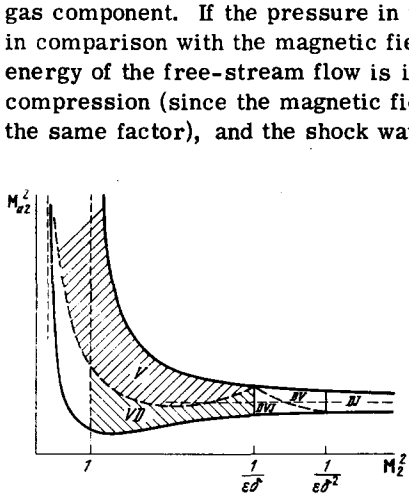

FIG. 9. Ranges of the Mach numbers ($\mathbf{M}_2^2$, $\mathbf{M}_{a2}^2$).

The shock adiabat for this case is given by Eq. (1.2) of Part II, where we should set $\alpha_1 = \alpha_2 = 1$.

Asymptotic analysis[78] is the method used to study the system of ordinary differential equations describing the shock layer. When we put this system of equations in dimensionless form, each physical process which can affect the front structure corresponds to a scale factor Δ_k (in the equations, these physical processes are described by the terms which contain derivatives with respect to x). For example, Joule heating corresponds to the scale length for magnetic-field diffusion; the current inertia corresponds to the collisionless penetration depth; etc. Defining the dimensionless coordinate ζ by $x = \Delta\zeta$ (Δ is some given scale), we find that all the derivatives appear with factors of the type Δ_k/Δ. In particular, if we treat the shock wave as a discontinuity of zero thickness or a "step" i.e., if we formally set $\Delta = \infty$, we find equations which contain no derivatives at all: specifically, the Rankine-Hugoniot algebraic relations, which relate the values of the variables ahead of and behind the shock wave. In studying the front structure we should choose the largest of the Δ_k. Let us assume for example, that the largest is Δ_1, i.e., that $\Delta_k/\Delta_1 \ll 1$ for $k \neq 1$. Then setting $\Delta = \Delta_1$, we can attempt to solve the equations in the zeroth approximation in the small parameters Δ_k/Δ_1. If we succeed in finding a continuous solution, which describes the transition from state 1 to state 2, then the process with the scale dimension Δ_1 is dominant in shaping the front structure, and the other processes can be treated as small corrections. If there is no such solution, it is necessary to introduce a new discontinuity, over a scale distance Δ_1, and to study its structure by the same method. This problem is frequently complicated by the need to take several processes into account simultaneously, when the corresponding scale lengths are comparable.

6. Shock waves in a magnetized plasma

We first consider the case of a pronounced anisotropy in the plasma transport coefficients, with magnetized ions and electrons, in other words, when the conditions $(\Omega_i\tau_i \gg 1, \Omega_e\tau_e \gg 1)$ hold over the entire shock front. We introduce $(\delta = (\Omega_i\tau_i)^{-1}$, and we will treat δ as a small parameter throughout this section of the paper.

In the equations for a shock layer with $\delta \ll 1$ we can distinguish the following processes and the corresponding scale lengths: $(\Delta_\nu = l/M)$ corresponds to ion viscosity, $\Delta_d = \varepsilon\delta Ml/M_a$ to electron inertia, $\Delta_j = \varepsilon\delta^2 Ml/M_a^2$ to Joule heating and Hall currents, and $\Delta_{rel} = Ml/\varepsilon$ to the temperature relaxation of the ions and electrons (l is the Coulomb mean free path). A comparison shows that Δ_{rel} is the largest of these scale lengths. Since the heat-transfer process is not itself responsible for either dissipation or dispersion, we conclude that in a shock layer narrow in comparison with Δ_{rel} the electrons and ions are heated independently, and beyond this layer is a relaxation zone with $v = \text{const}$, $H = \text{const}$, $T_e + T_i = \text{const}$ and[79]

$$x - x_0 = 0.91\frac{M_2^2 l_2}{\varepsilon}\left[\frac{1}{2}\ln\frac{1+(T_e/T_2)^{1/2}}{1-(T_e/T_2)^{1/2}} - \frac{1}{3}\left(\frac{T_e}{T_2}\right)^{3/2} - \left(\frac{T_e}{T_2}\right)^{1/2}\right]. \quad (6.1)$$

Since $\Delta_d \gg \Delta_j \sim \delta\Delta_d$, we can conclude that the ion viscosity and the dispersion due to electron inertia are the dominant factors in shaping the structure of the shock layer. The dispersion leads to the appearance of waves, and the waves are damped by viscous or Joule dissipation. Comparing Δ_ν and Δ_d, we see that ion viscosity is predominant in the case $M_2^2 \ll (\varepsilon\delta)^{-1}$; this region is marked V in Fig. 9. When $M_2^2 \gg (\varepsilon\delta)^{-1}$, the front structure is governed primarily by dispersion (region D in Fig. 9). In the case $\Theta_1^{5/2}(\varepsilon\delta)^{-1} \ll M_2^2 \ll (\varepsilon\delta)^{-1}$, the dispersion at the beginning of the shock front is more important than the viscosity (region VD). In the dispersion region, viscous dissipation is predominant if $M_2^2 \ll (\varepsilon\delta^2)^{-1}$, while the Joule loss is predominant if $M_2^2 \gg (\varepsilon\delta^2)^{-1}$ (subregions DV and DJ, respectively, in Fig. 9). In region V we find the following results within small terms of the order of ε and δ: The magnetic field is frozen in, $H/H_1 = N/N_1$; the electrons are heated only adiabatically, $T_e/T_1 = (N/N_1)^{2/3}$, and the heat conduction and Hall currents are suppressed by the strong transverse magnetic field. The solution of the equations for the shock layer in this approximation is $(\omega = v/v_1)$

$$\frac{T_i}{T_1} = 2 + \frac{4}{3}(1-\omega) + \frac{10M_1^2}{3}(1-\omega)\left(1 - \frac{1}{\omega M_{s1}^2}\right) - \frac{T_e}{T_1}, \quad (6.2)$$

$$x - x_0 = 0.3\frac{l_1}{M_1}\int_{[1+(N_1/N_2)]/2}^{\omega} \frac{[T_1(\omega')/T_1]^{5/2}\,d\omega'}{\omega'^2(\omega'-1)[\omega'-(N_1/N_2)](\omega'-\omega_{2-})}, \quad (6.3)$$

where ω_{2-} is the same as the right side of Eq. (5.1), except that the sign of the radical is changed. In the next approximation we can find the transverse velocity components of the ions and electrons,[71] which are small, on the order of δ.

The strongest transverse collisional shock waves which have been studied experimentally have been produced in the shock tube of the Plasma Physics Laboratory at Columbia University.[1,2,10,20,76,80-83] This device is a coaxial electromagnetic shock tube about 2 m long, in which transverse-shock velocities up to $4\cdot 10^8$ cm/sec have been reached in hydrogen at $p_1 = 50$ mtorr and $H_1 = 7.2$ kOe. The transverse magnetic field is produced by a current along the axis of the tube, so that the shock fronts are definitely not one-dimensional; their longitudinal section is approximately a parabola, curved toward the inner conductor. It is nevertheless meaningful to compare these experimental results with the results of the one-dimensional theory. In the case $M_1 \gg 1$ we can use (6.3) to find analytic estimates of the front thickness. Within terms $O(M_1^{-2})$, the Prandtl thickness is

$$L_{pr} \equiv \frac{v_1 - v_2}{|dv_i/dx|_{max}} = 2\sqrt{5}\,l_1.$$

Experimentally, however, it is not the front thickness "corresponding to maximum steepness" but the quantity $L_{exp} = \int_{v_{min}}^{v_{max}} dv\,|dv/dx|^{-1}$ which is measured. Here the difference between the velocity limits v_{min} and v_{max}, on the one hand, and the equilibrium velocities corresponding to the boundary conditions, on the other, is governed by the precision of the velocity measurements in the experiments. In the same approximation, we find from (6.3)

$$L_{exp} = \left(\frac{1}{32}\ln\frac{3}{4(v_2/v_1)_{min}-1} - 0.046\right)M_1^4 l_1. \quad (6.4)$$

(We note that $L_{exp} \gg L_{pr}$ at $M_1 \sim 10^2 - 10^3$!).

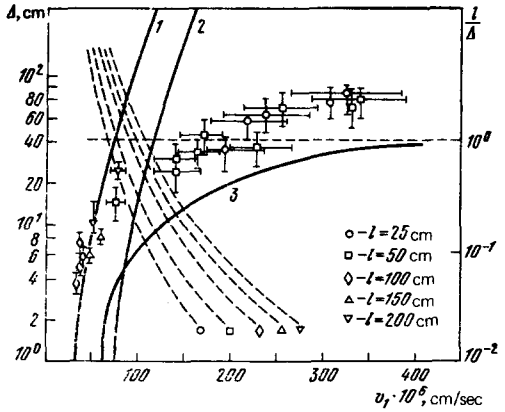

FIG. 10. Variation of the front thickness of a strong shock in a magnetized plasma with shock velocity v_1. The experimental points are from Ref. 76. Curve 1 is calculated from Eq. (6.4); curve 2 is the estimate of Ref. 5; curve 3 is the result of the numerical simulation of Ref. 4. The dashed curves show the distance from the beginning of the shock tube to the position of the detector, divided by the steady-state front thickness, calculated from (6.4).

Let us compare the theoretical results with the experimental data. The front thickness has been measured for strong shocks in magnetized plasmas by Moriette.[76] It is difficult to use Eq. (6.4) directly because the shock waves in these experiments were propagating through hydrogen at room temperature; i.e., they would be described better as ultrastrong ionizing shock waves. In order to correctly apply the purely plasma equation in (6.4) to an ionizing wave the most important point is to know the ion temperature correctly; the viscosity, which forms the front, is an extremely strong function of this temperature. We assume that there is initially a plasma with the same density of ions (protons) as in molecular hydrogen at $T = 300\,^\circ$K. We determine the "effective" Mach number M_{1eff} by using the equation for the plasma before the completion of the temperature relaxation, (6.1); adopting as the minimum velocity the lowest measured temperature in the experiments of Ref. 76, $T_1 = 100$ eV, we assume, in accordance with Ref. 5, that the error in the velocity determination is 1%. Figure 10 shows experimental points from Ref. 76, numerical results from Ref. 4, and estimates of the front thickness from Ref. 5 and Eq. (6.4) of the present paper.

According to the hydrodynamic description,[84] a stationary structure is formed only after the distance traversed by the shock wave is on the order of the steady shock thickness; then as a parameter to tell us whether the steady-state theory is applicable it is natural to adopt the ratio l/Δ, where l is the distance from the beginning of the shock tube to the detector, and Δ is the steady-state thickness for the given velocity, (6.4). We would expect the steady-state theory to agree with experiment in the case $l/\Delta > 1$ and to disagree in the case $l/\Delta < 1$. It can be seen from Fig. 10 that for all detector positions we find $l/\Delta < 1$ at $v_1 \gtrsim 10^8$ cm/sec. At lower velocities, there is a good agreement between the results of Ref. 76 and Eq. (6.4). The results of the numerical simulation in Ref. 4 agree with the experimental results even in the time-dependent case, thereby demonstrating the applicability of the hydrodynamic theory.

McNeill[82] has reported measurements of the electron temperature and density of the magnetic compression for the conditions $9\cdot10^6 < v_1 < 2\cdot10^7$ cm/sec, $H_1 = 1.0$ and 3.6 kOe. Calculating the expected magnetic compression H_2/H_1 from the measured velocity v_1 on the basis of (5.1), we find that the theoretical value of H_2/H_1 is 20–30% higher than the experimental values (the experimental error is about 15%). The slight discrepancy is apparently due to the fact that the shock waves in these experiments were not one-dimensional. Interestingly, the temperature relaxation corresponding to (6.1) was not observed in these experiments, although the shock wave traveled a distance large in comparison with Δ_{rel}. The electrons, heated to about 10 eV, can acquire a substantial amount of heat in collisions with ions, whose temperature is an order of magnitude higher, but the electron temperature does not increase. McNeill[82] believes that the reason is radiative cooling due to the strong resonant vacuum-UV emission of the multiply ionized atoms of heavy impurities, which are always present in the test gas (deuterium).

Independent measurements of the plasma compression N_2/N_1 and of the magnetic compression H_2/H_1 in Ref. 83, for velocities $10^7 < v_1 < 3\cdot10^7$ cm/sec, confirm the relation $H_2/H_1 = N_2/N_1$, within the experimental errors.

We turn now to another limiting case, in which the plasma behind the shock front is cold, i.e., $M_2^2 \gg (\varepsilon\delta)^{-1}$. In this case, Δ_d is the largest scale length. Setting

$$\Delta = \frac{1.05\varepsilon\delta M_2 l_2}{M_{a2}}$$

and omitting the terms which are small, of order ε, δ, or $(M_2^2\varepsilon\delta)^{-1}$, we find the following equations for the dimensionless magnetic field $h = H/H_1$ in the zeroth approximation (η is the Lagrange coordinate: $d/d\eta = (v/v_1)d/d\xi$):

$$\frac{1}{2}\left(\frac{dh}{d\eta}\right)^2 + \frac{(h-1)^2}{2}\left[\frac{(h+1)^2}{4M_{a1}^2} - 1\right] \equiv \frac{1}{2}\left(\frac{dh}{d\eta}\right)^2 + U(h) = 0, \quad (6.5)$$

$$\frac{d^2h}{d\eta^2} + (h-1)\left[\frac{h(h+1)}{2M_{a1}^2} - 1\right] = 0. \quad (6.6)$$

Equations (6.5) and (6.6) have a well-known mechanical analog[85-87]: the energy integral and the equation of motion of a particle of unit mass in a field $U(h)$. Obviously, Eqs. (6.5) and (6.6) cannot yield shock-wave solutions, since all the dissipative terms were discarded in the derivation of these equations. [At the front, there must be an increase in the entropy because of the irreversible conversion of the kinetic energy of the free-stream flow into heat. Attempts to find the front structure in the model of an ideal, dissipation-free medium—for example, in the plasma described by the Vlasov equation or, equivalently by the equations of motion of the components without collisions—are doomed to fail because of the very nature of the question, but, strange as it may seem, efforts along this line are still being published (see, for example, Ref. 88).] The boundary condition $h(-\infty) = 1$ singles out a soliton,

$$h(\eta) = 1 + \frac{2(M_{a1}^2 - 1)}{1 + M_{a1}\operatorname{ch}\left(2\eta\sqrt{1 - M_{a1}^{-2}}\right)}. \quad (6.7)$$

The maximum value $h = h_{max} = 2\mathbf{M}_{a1} - 1$ corresponds to the maximum density $N_{max} = N_1(2/\mathbf{M}_{a1} - 1)^{-1}$. The condition $N_{max} < \infty$ leads to the familiar relation

$$\mathbf{M}_{a1} < 2. \tag{6.8}$$

The meaning of this inequality is that in the case $\mathbf{M}_{a1} \geq 2$ the height of the potential barrier associated with the soliton is greater than the kinetic energy of the ions in the free-stream flow. Then a current of ions reflected from the soliton appears.

Even if we assume that this multiple-flow motion is laminar, the problem still goes beyond the scope of the model used here,[89,90] and we will not pursue it further.

If (6.8) holds, we can find a laminar hydrodynamic solution of the equations for the shock layer. The front structure will generally be oscillatory; the waves described by Eqs. (6.5) and (6.6) are damped in the next approximation because of the viscosity in parameter region DV and because of Joule dissipation in region DJ. In the intermediate case (region VD in Fig. 9) the scale length for the viscous dissipation, which increases rapidly with T_1, can be smaller at point 1 than the temperature-independent dispersion scale length, and it can be greater at point 2. There may thus be structures in which a finite number of waves at the bow part of the front precedes a monotonic approach to equilibrium behind the front.[72] We might note that weak shock waves always have a monotonic profile.

Another dispersion mechanism which is capable of imparting an oscillatory structure to transverse shocks in plasmas is charge separation.[86,90] For this to be a governing effect in the front structure, the following inequalities must hold[73]:

$$\max\left(\frac{l_1}{\mathbf{M}_1^2},\ r_{e1}\right) \ll r_{D1} \ll r_{l1}, \tag{6.9}$$

where r_{D1} is the Debye length, and r_{l1} and r_{e1} are the ion and electron gyroradii in state l.

The dispersion due to charge separation excites electrostatic oscillations of the cold ions with respect to the electrons, which are tied to the magnetic lines of force by the frozen-in condition [a deviation from this condition would mean that the electron inertia, which is negligible in the region defined by (6.9), would have to be taken into account]. The characteristic frequency is the ion plasma frequency, and the characteristic velocity is c_{a1}. In other words, the scale length for the effect is on the order of $c_{a1}/\omega_{pi} \sim r_{D_1}\beta_1^{-1/2} \gg r_{D_1}$ if[90] $\beta_1 \ll 1$.

It is not difficult to derive equations for the dimensionless ion velocity $\omega_i = v_i/v_1$ (in Lagrange coordinates, $d/d\eta = \omega_i d/d\zeta$, which are analogous to Eqs. (6.5) and (6.6):

$$\frac{1}{2}\left(\frac{d\omega_1}{d\eta}\right)^2 + \frac{1}{4}(\omega_1 - 1)^2\left[\frac{4}{\mathbf{M}_{a1}^2} - (\omega_1 + 1)^2\right] \equiv \frac{1}{2}\left(\frac{d\omega_i}{d\eta}\right)^2 + \tilde{U}(\omega_i) = 0, \tag{6.10}$$

$$\frac{d^2\omega_1}{d\eta^2} + (1 - \omega_1)\left[\omega_1(\omega_1 + 1) - \frac{2}{\mathbf{M}_{a1}^2}\right] = 0. \tag{6.11}$$

The magnetic field is $H = H_1[1 + \mathbf{M}_{a1}^2(1 - \omega_i^2)/2]$; the electron velocity is $v_e/v_1 = H_1/H$; and the electric potential is $\varphi = H_1(H - H_1)/4\pi e N_1$. The solutions of these equations are completely analogous to those discussed above. In particular, we can again construct a solution only under the condition $\mathbf{M}_{a1} < 2$. In addition to the similarity of these pairs of equations, there is also an important difference, which stems from the difference in the physical mechanisms for the two types of dispersion. In particular, in the mechanical analogy here the role of the equation of motion is played by the Poisson equation (above it was played by a generalized Ohm's law), while the energy integral is represented by the conservation equation for the plasma momentum (it was represented above by the energy conservation equation). This agreement of critical conditions is of course not simply fortuitous: These conditions are consequences of the conservation equations and they do not depend on the dispersion mechanism, just as the Rankine-Hugoniot conditions are independent of the nature of the dissipation.

In the case $\mathbf{M}_{a1} \geq 2$, there are no collisional hydrodynamic structures in region D (as yet, no systematic solutions have been derived for this case, even in the theory of collisionless shock waves). So far, no qualitative change in the structure at the transition through $\mathbf{M}_{a1} = 2$ has been observed experimentally (see Section 3 and the discussion below).

We emphasize that the physical role of charge separation in plasma shock waves is not simply one of exciting waves under condition (6.9). The charge-separation scale length in collisional hydrodynamics—the Debye length—is usually small in comparison with the front thickness, so that the assumption of a quasineutral plasma, which has been used consistently in this paper [except in (6.9)] is justified, but in this one-dimensional problem an extremely important result is the appearance, under the quasineutrality condition, of a strong axial field $E_x' \gg E_y$ ($\delta \ll 1$), which is directed perpendicular to the external magnetic field and to the current in the plasma (the Hall field). In the first place, this field creates a potential jump at the shock front, $\varphi_2 - \varphi_1 = \int_{-\infty}^{+\infty} E_x(\xi)d\xi$. In contrast with the jumps in all the other quantities, the jump $\varphi_2 - \varphi_1$ is not governed by the Hugoniot conditions (to some extent we have an analogy here with the boundary-condition problem discussed in Part I), and it depends directly on the front structure. From measurements of $\varphi_2 - \varphi_1$ we can learn about the mechanisms which operate to form the front structure (Section 7). In the second place, the presence of a Hall field masks the anisotropy of the conductivity,[74] so that when we ignore the electron inertia, the Hall currents, and so forth, Ohm's law takes the form $j_y = \sigma_\perp E_y$ in the present treatment, where the transverse conductivity is $\sigma_\perp \sim \sigma_\parallel$ (in a full ionized plasma, $\sigma_\parallel/\sigma_\perp \approx 2$). The deviation from a one-dimensional system in an actual experiment leads to the suppression of the transverse conductivity by the magnetic field, and this circumstance must be taken into account in calculating the Joule heating. For example, the heating of electrons to 10 eV in the experiments of Ref. 82, i.e., to a temperature much higher than the achieved in adiabatic compression, can be attributed to this small value of the transverse conductivity.

7. Shock waves in an unmagnetized plasma

We turn now to another limiting case: that of an unmagnetized plasma. In other words, we assume $(\Omega_i\tau_i)^{-1} = \delta \gg 1$ and also $(\Omega_e\tau_e)^{-1} = \varepsilon\delta \gg 1$. The following scale lengths arise in the equations: that for Joule dissipation, $\Delta_j = \varepsilon\delta^2 Ml/M_a^2$; that for the electron thermal conductivity, $\Delta_{T_e} = l/\varepsilon M^3$; that for the electron temperature relaxation, $\Delta_{rel} = Ml/\varepsilon$; and those for the ion viscosity and the ion thermal conductivity, $\Delta_{vi} = l/M$, $\Delta_{Ti} = l/M^3$. In the case $\varepsilon\delta \gg 1$, the largest of these lengths is Δ_j; this situation corresponds to a predominance of Joule dissipation. Here $\Delta_j \gg \Delta_{rel}$; i.e., in this case, a thermal equilibrium is reached between the plasma components ($T_e = T_i = T$) over a scale length Δ_j, within terms $O(\Delta_{rel}/\Delta_j)$. Ignoring the small terms of the order of ε and $(\varepsilon\delta)^{-1}$, we can use the energy and momentum conservation equations to express H and T in terms of the dimensionless velocity $\omega = v/v_1$:

$$\frac{H}{H_1} = \frac{1}{\omega} + \frac{3}{5\omega}\left[\sqrt{1 + \frac{40M_{a1}^2}{9}(\omega-1)(\omega-\omega_{2-})\left(\frac{N_2}{N_1}-\omega\right)} - 1\right], \quad (7.1)$$

$$\frac{T}{T_1} = 1 - \frac{M_i^2}{3\omega}(\omega-1)\left(\omega^2 + \omega - \frac{2}{M_{a1}^2}\right) - \frac{2M_i^2}{5\omega M_{a1}^2}\left[\sqrt{1 + \frac{40M_{a1}^2}{9}(\omega-1)(\omega-\omega_{2-})\left(\frac{N_2}{N_1}-\omega\right)} - 1\right]. \quad (7.2)$$

[Equations (7.1) and (7.2) of course remain valid under the subscript interchange 1 — 2. Equation (7.1) and (6.2), written in a different form: $\Phi(H/H_1, v/v_1) = 0$.]

The shock structure in the region in which Joule dissipation is predominant is governed by Ohm's law, which can be written as follows in our case of an unmagnetized plasma (scalar conductivity):

$$j_y = -\frac{c}{4\pi}\frac{dH_z}{dx} = \sigma\left\{E_y + \frac{1}{c}[\mathbf{vH}]_y\right\} = \frac{\sigma}{c}(v_1H_1 - vH).$$

Finally, in dimensionless form ($\xi = x/\Delta_j$), we have

$$\frac{vH}{v_1H_1} - 1 = 0.53\left(\frac{T}{T_1}\right)^{-3/2}\frac{d}{d\xi}\frac{H}{H_1}. \quad (7.3)$$

Using (7.1) and (7.2), we can integrate (7.3), finding an equation for the front structure in the form of an integral:

$$x - x_0 = 0{,}89\Delta_j \int_{[1+(N_2/N_1)]/2}^{\omega} d\omega' \frac{d}{d\omega'}\frac{H(\omega')}{H_1}\left[\frac{T(\omega')}{T_1}\right]^{-3/2} \times\left[\sqrt{1 + \frac{40M_{a1}^2}{9}(\omega'-1)(\omega'-\omega_{2-})\left(\frac{N_2}{N_1}-\omega'\right)} - 1\right]. \quad (7.4)$$

It is easy to see from (7.1) that the left side of (7.3) is positive for $N_2/N_1 < \omega < 1$; i.e., the sign of $dv/d\xi$ is governed by the sign of dH/dv along the curve (7.1). The solution (7.4) is meaningful only if $dH/dv < 0$. From Eq. (7.1) we easily find that this condition is met everywhere if $N_2/N_1 < \omega < 1$, provided that $M_2 > 1$; it is not met in a certain region $N_2/N_1 < \omega < \omega_4$ with $M_2 < 1$. In Fig. 3, the first case corresponds to the case in which both points 1 and 2 are on the supersonic branch of curve (2.2); in the second case, point 2 lies on the subsonic (lower) branch. In the first case, the predominant type of dissipation over the entire front is the Joule dissipation (a purely resistive structure); in the second case, the dissipation is not adequate for a continuous transition from 1 to 2, and an internal discontinuity must be introduced.[58] We note that in both cases the front thickness is governed by the Joule scale length (since the conductivity increases with the temperature, the Joule scale length is at a maximum in state 1, so that the front thickness is of the order of Δ_{j1}). This fact can be interpreted in the following way: The compressed magnetic field H_2 behind the front diffuses upstream in the free-stream flow, in which the conductivity is σ_1, for a distance on the order of $c^2/4\pi\sigma_1 v_1$.

Since $\Delta_{j1} \sim 1/v_1$, the magnetic structure of the Joule zone can be observed directly in weak shock waves, even in a plasma with a high initial conductivity.[91]

The appearance of an internal discontinuity at the front of a shock wave can also be derived by more formal methods, without going into detail on the structure of the shock front.[92,93] A simple physical explanation for the effect runs as follows: Joule heating can be responsible for the dissipation of an energy density on the order of $(H_2 - H_1)^2/8\pi$, where $H_2 \leq 4H_1$. In other words, the Joule dissipation is limited, while the kinetic energy density in the free-stream flow can be arbitrarily high. Consequently, beginning at some velocity v_1 (for a given β_1) the Joule dissipation becomes inadequate, and other dissipative processes must be called upon.[94] Figure 8 shows a curve of critical values of the Alfvén Mach number $M_a^h(\beta_1)$. Below $M_a^h(\beta_1)$, the structure of the shock waves is purely resistive; above this curve, there are shock waves with an internal discontinuity.

Since the internal discontinuity has a scale length $\Delta \ll \Delta_j$, we have $H = \text{const}$ in it to terms $O(\Delta/\Delta_j)$; in other words, *the discontinuity must be isomagnetic.*[58] As in Part II, it is simple to show that the only physically reasonable way to introduce this discontinuity is by means of an isomagnetic discontinuity in the stern part of the front ($h = H/H_1 = 1$; region 4–2 in Fig. 11). Since in the case $M_2 < 1$ we always have $M_2 \sim 1$ (Fig. 9), the scale lengths for the electron thermal conductivity and the electron-ion heat transfer are of the same order of magnitude, l_2/ε. The structure of the isomagnetic shock can be studied by setting $H = H_2$ and $\Delta = l_2/\varepsilon$.

The isomagnetic shock is a purely gas-dynamic effect, since in it we have $H = \text{const}$, and the only parameter which determines the intensity of this shock is the acous-

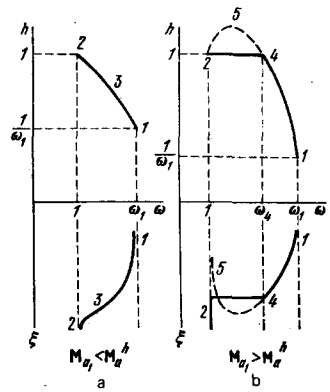

FIG. 11. Variation of $h = H/H_1$ with $\omega = v_2/v_1$ and $\omega(\xi)$ for $M_{a1} < M_a^h(\beta_1)$ (a) and $M_{a1} > M_a^h(\beta_1)$ (b).

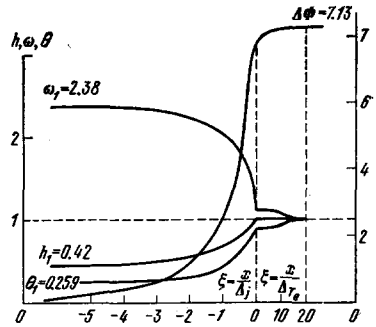

FIG. 12. Front structure of a shock wave with a slight isomagnetic shock. $M_1^2=20$, $M_{a1}^2=7$, $N_1=10^{16}$ cm^{-3}, $T_1=1$ eV, $H_1=1.4$ kOe.

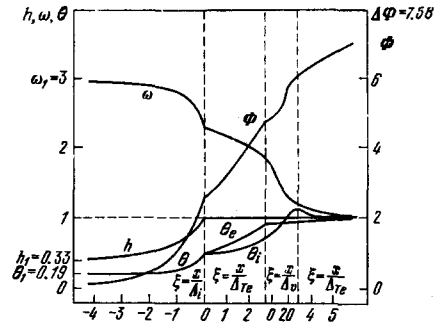

FIG. 13. Front structure of a shock wave with a strong isomagnetic shock. $M_1^2=17$, $M_{a1}^2=25$, $N_1=10^{16}$ cm^{-3}, $T_1=1$ eV, $H_1=0.68$ kOe. The scale dimensions of the isomagnetic shocks and of the electron isothermal shock have been enlarged for clarity. ($\omega=v/v_2$, $h=H/H_2$, $\theta_e=T_e/T_2$, $\theta_1=T_1/T_2$, $\Phi=e\varphi/kT_2$).

tic Mach number M_2. The structure of this shock is thus similar to that of a shock in a plasma without a magnetic field.[78, 95-98] From the conservation equations we can easily find the plasma velocity and temperature ahead of the isomagnetic shock (point 4):

$$\frac{v_4}{v_2}=\frac{M_2^2+3}{4M_2^2},\quad \frac{T_4}{T_2}=\frac{(M_2^2+3)(5M_2^2-1)}{16M_2^2},$$
$$M_4^2=\left[\frac{v_4}{c_s(4)}\right]^2=\frac{M_2^2+3}{5M_2^2-1}>1 \quad \text{for} \quad M_2^2<1. \tag{7.5}$$

The structure of the isomagnetic shock is the same as that of a shock without external fields in the case $M_1=M_4$ [the latter quantity is determined from the Mach numbers M_1 and M_{a1} of the original shock wave by means of Eqs. (5.1) and (5.2) and the obvious relation $M_2^2=(N_1/N_2)^2(T_1/T_2)M_1^2$]. Over the scale length $\Delta=0.316l_2/\varepsilon$, the structure is described by the equations ($\omega=v/v_2$)

$$\frac{d}{d\zeta}\frac{T_e}{T_2}=M_2^3\left(\frac{T_e}{T_2}\right)^{-5/2}(\omega-1)\left(\frac{v_4}{v_2}-\omega\right), \tag{7.6}$$

$$\frac{d\omega}{d\zeta}=\left\{\frac{d}{d\zeta}\frac{T_e}{T_2}+\frac{1,2}{M_2\omega^2}\left(\frac{T_e}{T_2}\right)^{-3/2}\left[\frac{T_e}{T_2}-\omega+\frac{5}{3}M_2^2\omega(\omega-1)\right]\right\}$$
$$\times\left[\frac{10}{3}-\frac{10}{3}M_2^2(8\omega-5)-\frac{2}{3\omega}\frac{T_e}{T_2}\right]^{-1}. \tag{7.7}$$

The second factor in (7.7) has the same sign at points 1 and 2 in the case $M_2^2>4/5$ ($M_4<1.12$) or different signs in the case $M_2^2<4/5$ ($M_4>1.12$). In the first of these cases, a slight isomagnetic shock is thus observed in the structure. It is formed by the electron thermal conductivity and it has a thickness

$$L_{Pr}\approx\frac{0.56l_2}{M_2(1-M_2^2)\varepsilon}.$$

This structure corresponds to Mach numbers in the range $M_2^A(\beta_1)<M_{a1}$ $M_2^T(\beta_1)$ (Fig. 8). Figure 12 shows front profiles calculated for a shock wave of intermediate intensity in a cold plasma (compression from 10^{16} to $2.4\cdot10^{16}$ cm^{-3}; heating from 1 to 3.9 eV).

If $M_2^2<4/5$, we must introduce yet another discontinuity within the isomagnetic shock. The structure of this new discontinuity is governed by the ion viscosity and thermal conductivity; the corresponding scale length is l_2. Within small terms of the order of ε, the electron temperature remains constant over this shock (the so-called electron isothermal discontinuity). The structure of this shock is extremely similar to that of a shock layer in a magnetized plasma; in both cases, the dissipation is due primarily to the viscosity which shapes a monotonic front profile. No restrictions of any kind are imposed on the intensity of the shock wave, because the viscosity is capable of any arbitrary dissipation level. The strong electron isothermal discontinuity divides the isomagnetic shock into two parts. In the first part, the electron temperature increases (to nearly the limiting value), and then the ion temperature and velocity change rapidly at the isothermal shock (the ion temperature rises above the limiting value). In the rest of the isomagnetic shock, there are a temperature relaxation and a slight compression due to the electron thermal conductivity (in Fig. 13, this structure is shown for a shock wave in which the plasma is compressed from 10^{16} to 10^{16} cm^{-3} and heated from 1 to 5.3 eV). As the intensity of the shock wave increases, a progressively larger part of the total jump in the density, temperature, and potential will be concentrated in this ion shock. Also noting that the plasme becomes magnetized as the temperature increases, regardless of the initial magnetic field, we can conclude that the structure of strong shock waves differs from that discussed in section 6 only in the presence of a small Joule region in the bow part of the front.

We turn now to yet another limiting case, whose range of applicability is narrower than for the cases above. This is the intermediate case of a partially magnetized plasma, in which the electrons are magnetized ($\Omega_e\tau_e\gg1$) but the ions are not[72] ($\Omega_i\tau_i\ll1$). Under these conditions, most of the dissipation is due to Joule heating, electron thermal conductivity, and Hall currents. The ions are heated adiabatically. It is clear from the discussion above that these dissipation mechanisms are not sufficient for very strong waves. An internal discontinuity, which is simultaneously isomagnetic and isothermal with respect to the electron temperature, appears at $M_2<M_{2cr}$, where M_{2cr} is the solution of the transcendental equation

$$M_2^2=\frac{1}{5}\left[3+\frac{T_1}{T_2}\left(\frac{N_2}{N_1}\right)^{2/3}\right].$$

In the limit $M_1\to\infty\beta_1\to0$, the corresponding critical Mach number is $M_{a1}=2\sqrt{3}=3.46$.

So far, few experimental results have been reported on shock waves in unmagnetized plasmas.[6] The expected thickness of the Joule wave is

$$\Delta_{J1}=\frac{2\cdot10^6}{v_{1cm/sec}T_{e1eV}^{3/2}}\left\{1+0.23\lg\left[T_{e1(eV)}^2\cdot\frac{10^{16}\text{cm}^{-3}}{n_{e1}}\right]\right\}. \tag{7.8}$$

(If only the electrons are magnetized in state 1, this quantity should be multiplied by two.) Under typical experimental conditions (in pinches and electromagnetic shock tubes) we have $N_1 \approx 10^6$ cm^{-3}, $T_{e1} \approx 1$ eV, $v_1 \approx 10^7$ cm/sec, and $\Omega_e \tau_e > 1$. In other words, the thickness of the shock front, Δ_{f1}, is on the order of 0.5 cm, in agreement with experiment.[6] It is difficult to interpret these experimental results because the deviation from a one-dimensional situation and the magnetic-flux loss are generally important in the corresponding experiments (not all the magnetic flux is compressed by the shock wave). Therefore, the order of magnitude of the front thickness is about the only measurable quantity which can be compared with the simplified theory. In Ref. 99, for example, with $N_1 = 10^{16}$ cm^{-3} and $T_{e1} = 1.2$–2.1 eV we find from (7.8) the value $\Delta_{f1} \approx 0.3$–0.6 cm for $v_1 = 2 \cdot 10^6$ cm/sec. This value corresponds to the measured values (0.3–0.8 cm). The loss of magnetic flux, however, substantially changes the flow pattern; for example, L_{exp} does not fall off in proportion to v_1^{-1}. On the contrary, it increases linearly with v_1. Sommer and Barach[99] explain their results by introducing phenomenological parameters to describe the deviation from an ideal apparatus.

Collisional Joule heating can be observed in shock waves in a low-density plasma ($N_1 \lesssim 10^{15}$ cm^{-3}), in which collisionless effects are important. Let us examine, for example, the experiments of Ref. 100, with $T_{e1} = 1$ eV, $N_1 = 7 \cdot 10^{14}$ cm^{-3}, $H_1 = 1200$ Oe, $M_{a1} = 2.5$, and $v_1 = 2.5 \cdot 10^7$ cm/sec. From (5.1) we find the expected magnetic compression to be $H_2/H_1 = 2.5$, in agreement with the measured results. An estimate of the rise time of the front on the basis of (7.8) yields 12 nsec, which is approximately the same as the observed rise time (about 10 nsec). Finally, an estimate of the electron and ion temperatures under the assumption of Joule heating of the electrons, without heat exchange,[101] yields $T_{e2} = 46$ eV and $T_{i2} = 2$ eV, in approximate agreement with the measured values.[102] The qualitative picture of the structure, however, shows that the collisional Joule heating, which is important in the bow region, gives way to different dissipation mechanisms. Even at $M_{a1} = 2.5$ the shock front is steeper at the beginning than at the end (the opposite should be true in a purely resistive shock wave). At $M_{a1} = 3.7$ (i.e., $M_2 < 1$), there is no resistive mechanism (neither the Coulomb nor anomalous resistance of the plasma) which could explain the necessary dissipation, as can be seen from the discussion above.[103] Correspondingly, the structure undergoes a qualitative change from the case $M_{a1} = 2.5$, but not as described above. The isomagnetic "step" does not appear just behind the Joule zone; instead, it appears in front of it. A study of structures of this type really belongs in the theory of collisionless shock waves, and much progress has been achieved in this field,[85–87,89,90,104,105] although the problem is clearly far from complete resolution. We would just like to say that ordinary Joule heating can also be important in structures of this type.

IV. CONCLUSION

As we mentioned in the Introduction, shock waves in magnetic fields are an extremely common phenomenon, with which physicists working in very different fields must deal. We have restricted the present review to the simplest case of transverse shock waves. This case is relatively simple to study because small perturbations propagate across the magnetic field only at the velocity of a fast magnetosonic wave, so that only fast shock waves exist. In the general case of an arbitrary orientation of the magnetic field with respect to the plane of the shock front, including the case of normal, enclosing shock waves,[106,107] the arguments are in the same spirit as in the present paper, although there are many interesting new details. We have seen that the traditional picture of shock waves as zero-thickness discontinuity surfaces breaks down for shock waves in magnetic fields. The shock fronts in this case have a clearly macroscopic structure; furthermore, knowledge of the structure of a shock front is frequenly necessary for interpreting observations.

Another example, which is instructive because of its methodological aspects, demonstrating the unity of physical science, is the theory of ionizing shock waves in a magnetic field. It has proved to be impossible to derive a successful theory for ionizing shock waves in classical hydrodynamics, without appealing to the theory of gas breakdown and without considering electromagnetic radiation.

On the other hand, we are still far from having a complete systematic theory for shock waves, including collisionless shock waves (and it may not be possible to derive such a theory at all). Such a theory should be based on the kinetic approach, and from this standpoint the hydrodynamic theory can be thought of as a first approximation, which allows us to distinguish some experimentally observable effects which are of purely hydrodynamic origin. In this regard, the theory of collisionless shock waves may also prove useful for deriving a theory of collisionless shock waves. For example, the oscillatory structure of shock fronts, which is believed to be peculiar to collisionless shock waves, also arises in collisional shock waves, as we showed in Part III of this review.

[1] R. Gross, Nucl. Fusion **15**, 729 (1975).
[2] R. A. Gross, "Some gas dynamic aspects of fusion plasmas," Twelfth Biennial Fluid Dynamics Symposium (Symposium on Advanced Problems and Methods in Fluid Dynamics), Bialowieza, Poland, 8-13 September 1975.
[3] S. H. Schneider, C. K. Chu, and B. P. Leonard, Phys. Fluids **14**, 1103 (1971).
[4] S. H. Schneider, Phys. Fluids **14**, 805 (1972).
[5] R. T. Taussig, Phys. Fluids **16**, 384 (1973).
[6] C. K. Chu and R. A. Gross, in: Fizika vysokotemperaturnoĭ plazmy (Physics of Hot Plasmas), Mir, Moscow, 1972, p. 262.
[7] R. A. Gross, in: Physics of High Energy Density (ed. P. Caldirola and H. Knoepfel), Academic Press, New York, 1971 (Russ. Transl., Mir, Moscow, 1974, p. 275).
[8] A. G. Eskov, R. Kh. Kurtmullaev, A. I. Malutin, and V. N. Semenov, in: Sixth European Conference on Controlled Fusion and Plasma Physics, JINR, Moscow, 1973, p. 595.
[9] A. M. M. Todd, Phys. Fluids **18**, 453 (1975).
[10] F. L. Sandel, M. Niimura, S. H. Robertson, and R. A. Gross, Phys. Fluids **18**, 1075 (1975).

[11]H. C. Lui and C. K. Chu, Phys. Fluids **18**, 1277 (1975).
[12]F. Sarder, in: Proc. of Ninth Intern. Shock Tube Symposium, Stanford University Press, Stanford, California, 1973, p. 556.
[13]E. L. Loubsky, S. G. Prakash, and D. Bershader, in: Proc. of Ninth Intern. Shock Tube Symposium, Stanford University Press, Stanford, California, 1973, p. 568.
[14]M. Shiraishi, J. Phys. Soc. Jpn **39**, 1069 (1975).
[15]M. Ambar, K. S. Upadhyaya, and H. C. Khare, Nuovo Cimento **B34**, 47 (1976).
[16]S. G. Zaĭtsev and A. V. Mikhaĭlov, Dokl. Akad. Nauk SSSR **226**, 81 (1976) [Sov. Phys. Dokl. **21**, 24 (1976)].
[17]R. A. Glatman, Zh. Tekh. Fiz. **43**, 2115 (1973) [Sov. Phys. Tech. Phys. **18**, 1329 (1974)].
[18]R. M. Patrick, Phys. Fluids **2**, 589 (1959).
[19]W. B. Kunkel and R. A. Gross, in: Plasma Hydromagnetic (ed. D. Bershader), Stanford Univ. Press, Stanford, California, 1962, p. 58.
[20]R. A. Gross and B. Miller, in: Methods of Experimental Physics, Vol. 9, Part A (ed. H. R. Griem and R. H. Lovberg), Academic Press, New York, 1970, p. 169.
[21]A. I. Akheizer, I. A. Akheizer, R. V. Polovin, A. G. Sitenko, and K. N. Stepanov, Élektrodinamika plazmy (Plasma Electrodynamics), Nauka, Moscow, 1974.
[22]G. A. Lyubimov, Dokl. Akad. Nauk SSSR **126**, 291 (1959) [Sov. Phys. Dokl. **4**, 510 (1959–60)].
[23]C. K. Chu, Phys. Fluids **7**, 1349 (1964).
[24]R. T. Taussig, Phys. Fluids **10**, 1145 (1967).
[25]A. G. Kulikovskiĭ, Prikl. Mat. Mekh No. 6, 1126 (1968).
[26]M. I. Hoffert, Phys. Fluids **11**, 77 (1968).
[27]G. C. Vlases, J. Fluid Mech. **16**, 82 (1963).
[28]G. C. Vlases, Phys. Fluids **7**, 1358 (1964).
[29]G. C. Vlases, Phys. Fluids **10**, 2351 (1967).
[30]C. F. Stebbins and G. C. Vlases, J. Plasma Phys. **2**, 633 (1968).
[31]R. M. Patrick and E. R. Pugh, Phys. Fluids **8**, 636 (1965).
[32]A. L. Velikovich and M. A. Liberman, Zh. Eksp. Teor. Fiz. **74**, 1650 (1978) [Sov. Phys. JETP **47**, 860 (1978)].
[33]P. A. Maksimov and V. E. Ostashev, Teplofiz. Vys. Temp. **13**, 644 (1975).
[34]A. L. Velikovich and M. A. Liberman, Zh. Eksp. Teor. Fiz. **73**, 891 (1977) [Sov. Phys. JETP **46**, 469 (1977)].
[35]Ya. B. Zel'dovich and Yu. P. Raĭzer, Fizika udarnykh voln i vysokotemperaturnykh gidrodinamicheskikh yavleniĭ, (Physics of Shock Waves and High-Temperature Hydrodynamic Phenomena), Nauka, Moscow, 1966 [Academic Press, New York, 1966].
[36]B. P. Leonard, J. Plasma Phys. **17**, 69 (1977).
[37]M. A. Liberman and A. L. Velikovich, Plasma Phys. **20**, 439 (1978).
[38]H. D. Weymann, Phys. Fluids **3**, 545 (1960).
[39]T. G. McRae and B. M. Leadon, Phys. Fluids **15**, 2067 (1972).
[40]G. Kamimoto and K. Neshima, Trans. Jpn. Soc. Aeronaut. and Space Sci. **15**, 124 (1972).
[41]A. R. Viñolo and J. H. Clarke, Phys. Fluids **16**, 1612 (1973).
[42]A. C. Pipkin, Phys. Fluids **6**, 1382 (1963).
[43]H. D. Weymann, Phys. Fluids **12**, 1193 (1969).
[44]L. B. Holmes and H. D. Weymann, Phys. Fluids **12**, 1200 (1969).
[45]M. J. Lubin and E. L. Resler, Jr., Phys. Fluids **10**, 1 (1967).
[46]S. S. R. Murty and P. Serou, Phys. Fluids **15**, 1035 (1972).
[47]J. I. Mills, M. Naraghi, and R. G. Fowler, Phys. Fluids **17**, 691 (1974).
[48]H. F. Nelson, AIAA J. **13**, 115 (1975).
[49]M. Pinegre, Thesis, L'Universitet de Rouane, 1975.
[50]R. A. Dobbins, AIAA J. **8**, 407 (1970).
[51]R. Munt, R. S. B. Ong, and D. L. Turcotte, Plasma Phys. **11**, 739 (1969).
[52]É. D. Lozanskiĭ and O. B. Firsov, Teoriya iskry (Theory of the Spark), Atomizdat, Moscow, 1975.
[53]H. Petschek and S. Byron, Ann. Phys. (N.Y.) **1**, 270 (1957).
[54]H. Ezumi, Y. Enomoto, and M. Kawamura, J. Phys. Soc. Jpn. **32**, 1676 (1972).
[55]H. Ezumi, M. Kawamura, and T. Yokota, J. Phys. Soc. Jpn. **43**, 1060 (1977).
[56]F. de Hoffman and E. Teller, Phys. Rev. **80**, 692 (1950).
[57]H. L. Helfer, Astrophys. J. **117**, (1953).
[58]W. Marshall, Proc. R. Soc. London, Ser. A **233**, 367 (1955).
[59]H. K. Sen, Phys. Rev. **102**, 5 (1956).
[60]G. S. Golitsyn and K. P. Stanyukovich, Zh. Eksp. Teor. Fiz. **33**, 1417 (1957) [Sov. Phys. JETP **6**, 1090 (1958)].
[61]G. S. S. Ludford, J. Fluid Mech. **5**, 67 (1959).
[62]A. G. Kulikovskiĭ and G. A. Lyubivmo, Prikl. Math. Mekh. **23**, 868 (1959).
[63]S. B. Pikel'ner, Zh. Eksp. Teor. Fiz. **36**, 1536 (1959) [Sov. Phys. JETP **36**, 1089 (1959)].
[64]G. A. Lyubimov, Prikl. Mat. Mekh. **25**, 179 (1961).
[65]A. G. Kulikovskiĭ and G. A. Lyubimov, Magnitnaya gidrodinamika (Magnetohydrodynamics), Fizmatgiz, Moscow, 1962.
[66]J. E. Anderson, Magnetohydrodynamic Shock Waves, MIT Press, Cambridge, Mass., 1963 (Russ. Transl., Atomizdat, Moscow, 1968).
[67]W. Geiger, H. J. Kaeppeler, and B. Mayser, Nucl. Fusion Suppl. Part 2, 403, 1962.
[68]P. N. Hu, Phys. Fluids **9**, 89 (1966).
[69]H. Grad and P. N. Hu, Phys. Fluids **10**, 2596 (1967).
[70]P. N. Hu and H. Grad, Phys. Fluids **15**, 402 (1972).
[71]A. L. Velikovich and M. A. Liberman, Fiz. Plazmy **2**, 334 (1976) [Sov. J. Plasma Phys. **2**, 182 (1976)].
[72]A. L. Velikovich and M. A. Liberman, Zh. Eksp. Teor. Fiz. **71**, 1390 (1976) [Sov. Phys. JETP **44**, 727 (1976)].
[73]A. L. Velikovich and M. A. Liberman, Izv. Akad. Nauk SSSR, Mekhan. Zhidk. i Gaza No. 3, 134 (1977).
[74]S. I. Braginskiĭ, in: Voprosy teorii plazmy [Reviews of Plasma Physics (ed. M. A. Leontovich), Vol. 1, Consultants Bureau, New York, 1965], Vol. 1, Atomizdat, Moscow, 1963, p. 183.
[75]L. Spitzer, Physics of Fully Ionized Gases, Interscience, New York, 1956 (Russ. Transl., Mir, Moscow, 1965).
[76]P. R. Moriette, Phys. Fluids **15**, 51 (1972).
[77]L. D. Landau and E. M. Lifshitz, Élektrodinamika sploshnykh sred (Fluid Mechanics), Gostekhizdat, Moscow, 1957 [Addison—Wesley, Reading, Mass., 1959].
[78]M. Y. Jaffrin and R. F. Probstein, Phys. Fluids **7**, 1658 (1964).
[79]V. D. Shafranov, Zh. Eksp. Teor. Fiz. **32**, 1453 (1957) [Sov. Phys. JETP **6**, 1183 (1957)].
[80]E. Halmoy, Phys. Fluids **14**, 2134 (1971).
[81]R. A. Gross, Cited on p. 72 in Ref. 12.
[82]D. H. McNeill, Phys. Fluids **18**, 44 (1975).
[83]S. Robertson and Y.-G. Chen, Phys. Fluids **18**, 917 (1975).
[84]M. J. Lighthill, in: Surveys in Mechanics (ed. G. K. Batchelor and R. M. Davies), Cambridge Univ. Press, Cambridge, Mass., 1956, p. 250.
[85]R. Z. Sagdeev, in: Voprosy teorii plazmy [Reviews of Plasma Physics (ed. M. A. Leontovich), Vol. 4, Consultants Bureau, New York, 1966], Vol. 4, Atomizdata, Moscow, 1964, p. 20.
[86]D. Tidman and N. A. Kroll, Shock Waves in Collisionless Plasmas, Wiley Press, New York, 1971.
[87]V. I. Karpman, Nelineĭnye volny b dispergiruyushchikh sredakh (Nonlinear Waves in Dispersive Media), Nauka, Moscow, 1973.
[88]R. E. Meyer, in: Nonlinear Waves (ed. S. Leibovich and A. R. Seebass), Cornell Univ. Press, Ithaca, New York, 1974 (Russ. Transl., Mir, Moscow, 1977, p. 244).
[89]D. Sherwell and R. A. Cairns, J. Plasma Phys. **17**, 265 (1977).
[90]A. A. Galeev and R. Z. Sagdeev, Cited in Ref. 85, Vol. 7, 1973, p. 3.
[91]V. Čadež and S. Selak, Fizika **6**, 67 (1974).
[92]G. B. Whitman, Comm. Pure Appl. Math. **12**, 113 (1959).

[93]V. S. Imshennik, Fiz. Plazmy **1**, 202 (1975) [Sov. J. Plasma Phys. **1**, 108 (1975)].
[94]E. Hintz, Cited on p. 213 in Ref. 20.
[95]M. S. Greywall, Phys. Fluids **18**, 1439 (1975).
[96]M. S. Grewal (*sic*), Phys. Fluids **16**, 561 (1973).
[97]M. S. Greywall, Phys. Fluids **19**, 2046 (1976).
[98]V. S. Imshennik, Zh. Eksp. Teor. Fiz. **42**, 236 (1962) [Sov. Phys. JETP **15**, 167 (1962)].
[99]E. J. Sommer, Jr., and J. P. Barach, Phys. Fluids **14**, 2102 (1971).
[100]J. W. M. Paul, L. S. Holmes, M. J. Parkinson, and J. Sheffield, Nature **208**, 133 (1965).
[101]D. L. Morse, Plasma Phys. **15**, 1262 (1973).
[102]J. W. M. Paul, G. C. Goldenbaum, A. Iiyoshi, L. S. Holmes, and R. A. Hardcastle, Nature **216**, 363 (1976).
[103]M. Kornherr, Z. Phys. **233**, 37 (1970).
[104]L. C. Woods, J. Plasma Phys. **3**, 435 (1969).
[105]W. M. Manheimer and I. Haber, Phys. Fluids **17**, 706 (1974).
[106]M. A. Liberman, Zh. Eksp. Teor. Fiz. **75**, 1652 (1978) [Sov. Phys. JETP **48**, 832 (1978)].
[107]M. A. Liberman, Zh. Eksp. Teor. Fiz. **77**, 124 (1979) [Sov. Phys. JETP **50**, 63 (1979)].
[108]B. P. Leonard, J. Plasma Phys. **10**, 13 (1973).
[109]B. P. Leonard, J. Plasma Phys. **7**, 157 (1972).

Translated by Dave Parsons
Edited by Morton Hamermesh